

Subchannel Notching and Channel Bonding: Comparative Analysis of Opportunistic Spectrum OFDMA Designs

Jihoon Park, Przemysław Pawełczak, Pål Grønsund, and Danijela Čabrić

Abstract

We present an analytical model that enables a comparison of multiple design options of Opportunistic Spectrum Orthogonal Frequency Division Multiple Access (OS-OFDMA). The model considers continuous and non-continuous subchannel allocation algorithms, as well as different ways to bond separate non-continuous frequency bands. Different user priorities and channel dwell times, for the Secondary Users and the Primary Users of the radio spectrum, are studied. Further, the model allows the inclusion of different types of Secondary User traffic. Finally, the model enables the study of multiple two-stage spectrum sensing algorithms. Analysis is based on a discrete time Markov chain model which allows for the computation of network characteristics such as the average throughput. From the analysis we conclude that OS-OFDMA with subchannel notching and channel bonding could provide, under certain network configurations, almost seven times higher throughput than the design without those options enabled.

I. INTRODUCTION

One of the ways to combat artificial spectrum scarcity [2] is to augment existing radio access techniques with Opportunistic Spectrum Access [3], [4] (OSA). Wireless networks with OSA capabilities are able

Jihoon Park, Przemysław Pawełczak, and Danijela Čabrić are with the Department of Electrical Engineering, University of California, Los Angeles, 56-125B Engineering IV Building, Los Angeles, CA 90095-1594, USA (email: {jpark, przemek, danijela}@ee.ucla.edu).

Pål Grønsund is with the Telenor, Snarøyveien 30, 1331 Fornebu, Norway; Simula Research Laboratory, Martin Linges Vei 17, 1364 Fornebu, Norway; and the Department of Informatics, University of Oslo, Gaustadallen 23, 0373 Oslo, Norway (email: pal.gronsund@telenor.com).

Part of this work has been accepted to the proceedings of IEEE GLOBECOM, Dec. 6–10, 2010, Miami, FL, USA [1].

to search for unused portions of the radio spectrum and communicate over vacant radio frequencies whenever the assigned radio capacity is insufficient.

Orthogonal Frequency Division Multiple Access (OFDMA) is a multiple access technique where frequency subchannels, composed of orthogonal subcarriers, are assigned to individual users of the network. Subchannel assignment is usually performed by a central entity, often the Base Station (BS), and can be based on the quality of service requirements of the individual users. Because of high spectral efficiency, ability to allocate non-continuous subchannels (in the frequency domain) to a single user, as well as robustness against inter-symbol interference and time synchronization errors, OFDMA was a design choice of such recent wireless networking standards as IEEE 802.16 [5], IEEE 802.20 [6] and 3GPP Long Term Evolution [7]. Thus, it is natural to think of combining the strengths of OFDMA with the flexibility of OSA [8].

Most papers analyzing the performance of opportunistic spectrum OFDMA (OS-OFDMA) systems are too specific, focusing on one feature of the system in isolation from the rest of the network protocol stack. For example, many recent papers have proposed optimal OFDMA resource allocation in the OSA scenario, for instance refer to a recent work of [9]. However, it has been usually assumed that information about channels occupied by PU was known a priori and traffic characteristics and priority levels of SU were not considered. In [10] a general evaluation framework for IEEE 802.16 with OSA capabilities has been proposed. The paper focused mostly on propagation calculations, including coverage, interference and protection distances with a very simplified networking model used, based on Erlang-B formula [10, Sec. V-A]. Lastly, authors in [11] have analyzed OSA-based OFDMA network with the focus on resource allocation, with one class of OSA traffic and a static licensed user.

Presumably the first formal proposal of using OFDMA in OSA scenario was the IEEE P802.22 standard [12], [13]. In [14] the IEEE P802.22-like network has been evaluated using only simulations with a very limited set of scenarios. We are not aware of any paper that have focused on cohesive analysis of IEEE P802.22, that would take into account its intrinsic features, including multiple classes of traffic, two stage spectrum sensing, different levels of PUs and their temporal activity, OFDMA subcarrier allocation process and channel and subchannel management strategies. Such types of analysis have been comprehensively performed in [15] to evaluate IEEE 802.16 network, but obviously they could not be used directly to evaluate OS-OFDMA network due to the lack of spectrum sensing and incumbent users activity analysis. Moreover, due to the big number of design options for OS-OFDMA, the literature lacks a comparative framework for different schemes of OS-OFDMA.

Therefore, in this paper we propose an analytical framework to evaluate the performance of networks

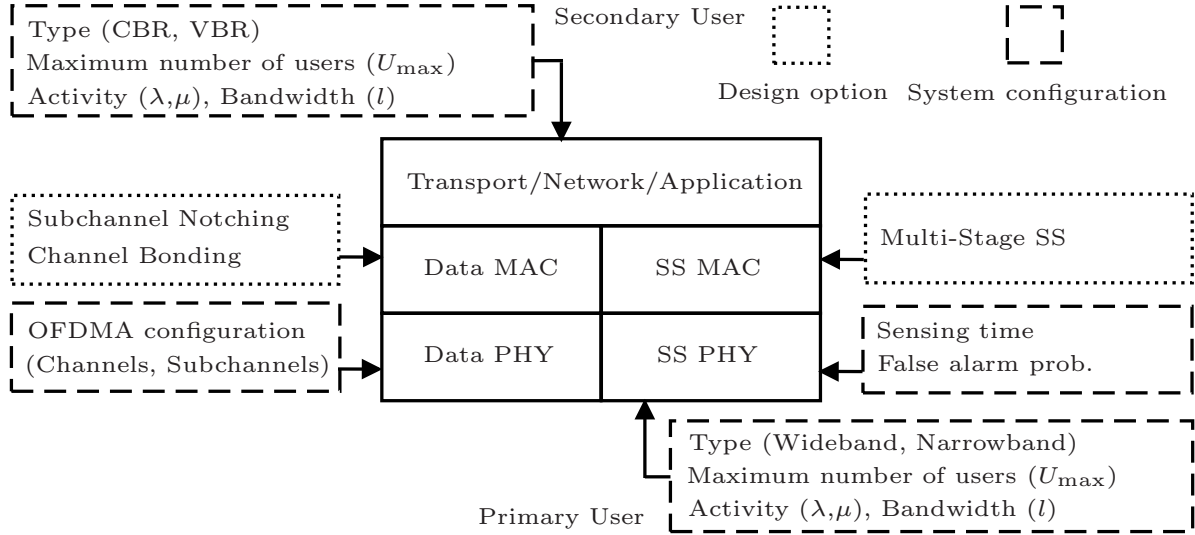


Fig. 1. OS-OFDMA system model; SS: spectrum sensing.

based on OS-OFDMA, considering multiple protocol functionalities and features that are mostly specific to OFDMA. That is, we consider different channelization structures, subchannel allocation algorithms, resource assignment strategies and different spectrum sensing methods. Furthermore, in the model we consider different priorities and channel dwell times of Secondary Users (SUs) and Primary Users (PUs) of the spectrum.

The rest of the paper is organized as follows. A system model outlining OS-OFDMA network design options in detail is presented in Section II. An analytical model for evaluating throughput of the considered system is presented in Section III. Numerical results follow in Section IV. The paper is concluded in Section V.

II. SYSTEM MODEL

We consider a centrally controlled network with OS-OFDMA, where a BS manages resources of individual network subscribers. Although the proposed model is applicable to both uplink and downlink traffic, for simplicity we assume that only downlink traffic is transmitted. In this paper, we constrain ourselves to a single cell configuration with multiple SUs and multiple PUs, belonging to different user classes. This allows the isolation of the effects of co-channel and adjacent channel interference, as well as co-existence mechanisms in OSA network on the investigation of the relation between PU type, its activity level and OS-OFDMA design options. Further, transmission errors on the subchannels are considered.

A model of the OSA protocol stack under consideration is depicted in Fig. 1. We identify two main modules: (i) data transmission, which is responsible for regular data communication between SUs, and (ii) spectrum sensing, which is responsible for efficient detection of spectrum opportunities for the OSA network; see also [16] for a similar model. Each component has its unique physical (PHY) and medium access control (MAC) layer. Obviously each layer has its unique design options, like channel and subchannel management algorithms and multi-stage sensing. Also OSA network can be described by individual parameters such as type of traffic transmitted, activity level and bandwidth used. In Section II-A we introduce the physical layer OS-OFDMA configurations considered in this paper. Later in Section II-B we introduce the spectrum sensing and MAC design options of interest. We aim to calculate the average throughput obtained at the data MAC layer for all classes of SU traffic.

A. OSA System Configuration

1) *Channel Setup and its Relation to OFDMA*: The frequency domain consists of X channels, each of which is composed of Y OFDMA subchannels. The total number of subchannels is thus $M = XY$ (note that all variables used in the paper are summarized in Table I). Each subchannel is further composed of OFDM subcarriers. In this paper, we constrain ourselves to subchannel domain analysis. Furthermore, we assume that subchannel throughput C is constant, while its value depends on the physical layer characteristics such as modulation, error control coding, and MAC layer overhead such as the OFDMA preamble length.

In the time domain, transmission segments are divided in frames of length t_f . At the beginning of each frame, SUs of OSA network detect the presence of the PU. We implicitly assume a synchrony between PU and SU activity, as it is a well established assumption in the theoretical analysis, see [16] for a large collection of recent publications that follow the same path. Furthermore, we assume that each node in the OSA network observes the same signal emitted by the PU, thus each SU performs all the sensing measurements alone and sends the measurement result to BS on the uplink. Then, BS makes a final decision about the presence of PU on each subchannel.

2) *PU and SU Types*: We consider different types of PUs and SUs. For the PUs, depending on the bandwidth and the activity level, we classify them into: (i) a wideband PU (WPU) having low activity, i.e. with long busy and long idle times, and (ii) a narrowband PU (NPU) having high activity, i.e. with short busy and shorter than WPU idle times. This classification makes the analysis more detailed and realistic. It also makes different scenarios of interest possible to analyze. For example, WPU can represent wireless video links, while NPU can represent wireless microphones, both operating in the TV bands.

TABLE I
SUMMARY OF SYMBOLS USED IN THE PAPER

Variable	Description	Unit
b, θ	Subchannel bandwidth and sensing threshold	Hz, —
$w, n, c, v, a (f)$	Index: WPU, NPU, CBR, VBR, coarse (fine) sensing	—
x, y, i, j, k, r	Supporting variables	—
$1/h, v$	Number of inhabitants per active NPU, user speed	—, mph
$m_x (l_x)$	Number of subchannels used by (assigned to) user x	—
t_f	Frame length	s
$t, x^{(t)}$	Time stamp, variable x at time t	—
C, C_p	Throughput: subchannel, MAC layer subchannel	bps
H, H_x	Throughput: total, obtained by connection type x	—
M, M_a	Number of subchannels: total, detected as idle	—
M_m, M_p, M_0	Number of subchannels: mis-detected, used by PU, detected as idle	—
X, X_n, X_a	Number of channels: total, used by PU, detected as idle	—
$U_x, U_{x,\max}$	Number of users: type x , type x maximum	—
U_a	Number of CBR users able to utilize all subchannels	—
U_{e1}, U_{e2}	Supporting variables denoting number of NPUs	—
Y	Number of subchannel per channel	—
S	Two-stage sensing option indicator	—
F, V	Supporting variable to compute: $\text{Pr}_{14}(\cdot)$, $\text{Pr}_{25c}(\cdot)$	—
L	BS cell diameter	mi
1_c	Indicator function for feasible conditions of $\text{Pr}_{20}(\cdot)$	—
p_{10}, p_{11}	Probability for single SU node: false alarm, detection	—
$\text{Pr}_x(\cdot)$	Expressions to calculate average throughput	—
$f_+(\cdot), f_s(\cdot)$	Supporting function to compute: $\text{Pr}_2(\cdot)$, $\text{Pr}_{21}(\cdot)$	—
$H, J^{(y)}$	Supporting function to compute: $\text{Pr}_{25}(\cdot)$, $\text{Pr}_{25x}(\cdot)$	—
$G_x(\cdot), T_x(\cdot)$	Probability: connection generation, connection termination (type x)	—
$\mathcal{K}_{c,a}, \mathcal{K}_{c,b}, (\mathcal{K}_v)$	Vectors of possible i, j for $U_c^{(t)}$ ($U_v^{(t)}$)	—
$\mathcal{K}_{n,a}, \mathcal{K}_{n,b}, (\mathcal{K}_w)$	Vectors of possible i, j for $U_n^{(t)}$ ($U_w^{(t)}$)	—
$\mathcal{M}, \mathcal{U}, \mathcal{S}$	Sets: $\{U_c, U_v, M_a\}$, $\{U_w, U_n\}$, $\{S, U_w, U_n\}$	—
$\mathcal{X}, \mathcal{Y}, \mathcal{Z}$	Sets: $\{X_n\}$, $\{0, \dots, M\}$, $\{Y, \dots, M\}$	—
$\mathcal{I}(\cdot)$	Supporting set to compute $f_s(\cdot)$	—
$1/\lambda_x, 1/\mu_x$	Average time: departure, arrival (type x)	s
$\delta_x, \phi_x (\tau_x)$	Probability: false alarm, detection (sensing) time (stage x)	—
ξ, η	MAC overhead, average ratio of data transmission to total frame length	—
ρ	Population density	—
\mathbb{N}, \mathbb{R}	Number sets: natural, real	—

For SU, again making our framework general and applicable to multiple scenarios, we consider two types of users: (i) those receiving real-time traffic, denoted as the constant bit rate (CBR) SUs, and (ii) those receiving elastic traffic, denoted as variable bit rate (VBR) SUs. In our OSA network model, different types of SU traffic flows are generated at the upper layers, i.e. application, network and transport, and forwarded down to data PHY, while PU signals are detected at the spectrum sensing module, see Fig. 1.

Furthermore, we assume that the system has a hierarchical structure such that the WPU has the highest priority in accessing bandwidth, NPU is the second in access hierarchy, followed by CBR and finally VBR. In other words, if users of different classes access the same subchannel, the lower priority class user must vacate in order for the higher class user to utilize the subchannel. The evacuated CBR switches to the other idle subchannels or drops the connection if there is no idle subchannel available. For VBR, if the PU is detected, the active VBR connection squeezes the bandwidth [15, Sec. III-B] excluding the channel or subchannel occupied by the PU, and if there is no channel detected as idle, it buffers data until the PU disappears. Note that the behavior of VBR promises to obtain highest possible throughput, as demonstrated in [16, Sec. V-B and Fig. 6], assuming no switching overhead, while CBR does not consider buffering due to the excessive delay that this class might experience while waiting for WPU or NPU to vacate the bandwidth.

Because of the finite channel capacity, the number of users considered in the system is finite, but different for different user types. We assume that at most $U_{w,\max}$, $U_{n,\max}$, $U_{c,\max}$ and $U_{v,\max}$ of WPUs, NPUs, CBR and VBR connections, respectively, can be active at the same time in the considered bandwidth [15, Sec. III-B]. For the data traffic of SUs and PUs, for analytical tractability, we assume that all users generate new connections according to the negative exponential distribution for the inter-arrival time and burst departure time¹. The average inter-arrival and departure time are denoted, respectively, as $1/\lambda_w$ and $1/\mu_w$ for WPU, $1/\lambda_n$ and $1/\mu_n$ for NPU, $1/\lambda_c$ and $1/\mu_c$ for CBR, and $1/\lambda_v$ and $1/\mu_v$ for VBR. Also we assume that connection of each class except for VBR occupies a fixed number of subchannels. We denote the instantaneous number of subchannels utilized by a connection class as l_w for WPU, l_n for NPU, l_c for CBR and l_v for VBR. Note that the number of subchannels assigned to every connection is fixed and $l_c, l_w, l_n \in \mathbb{N}$, except for a VBR connection. In that case $l_v \in \mathbb{R}$, which stems from the fact that one data frame consists of a group of OFDMA symbols and the symbols in

¹The analysis can be extended to the general distributions of PU and SU traffic, which is beyond the scope of this paper. Note, however, that the recent measurement campaign [17] showed that more than 60% of measured PU activities distributions, including ISM and cellular bands, fitted an exponential distribution.

the OFDMA frame can be assigned to multiple VBR connections. Also, for VBR connections, the burst departure time depends on the number of subchannels used by VBR, thus $1/\mu_v$ is an average departure time when one subchannel is assigned to the VBR connection.

B. Design Options

1) *Spectrum Sensing PHY and MAC Layers*: Sensing PHY senses the PU signal on the channel and passes the measurement about subchannel availability to the sensing MAC layer for further processing. When a PU is present on the subchannel, it transmits a signal with a certain power and/or unique feature. Thus by detecting the power and/or the feature, the SU can decide whether the PU signal is on the subchannel or not. The main parameters for the spectrum sensing PHY are the probability of detection, the probability of false alarm and the sensing time. There is a trade-off between the sensing time and the resulting probabilities [18]. That is, if a SU takes a long time to sense a subchannel, the time for data transmission may be reduced. However, more idle subchannels can be detected because of high accuracy, which in turn may increase bandwidth utilization. Therefore sensing time and sensing accuracy are the critical design options for the sensing PHY.

In the sensing MAC layer, the SUs decide collectively, with the help of BS, on the state of the PU state on the subchannel based on the sensing results of the sensing PHY. We denote the detection based on multiple users as collaborative sensing and that based on multiple periods as multi-stage sensing. Since the performance of collaborative sensing is relatively well known, see for example [16], in this paper, we focus mostly on multi-stage sensing². For the first results of multi-stage spectrum sensing in network context refer to [20] for two-stage sensing multi-channel system, and [21] for two-stage sensing single channel system.

In this work we limit ourselves to two-stage sensing, noting that our analysis can be directly extended to multi-stage sensing. The procedure works as follows. First, the SU senses the subchannel coarsely at the beginning of every frame, with short sensing time and low sensing accuracy. If the PU is detected, the SU switches to fine sensing mode (immediately, in the same frame), with long sensing time and high sensing accuracy. Depending on the sensing strategy, fine sensing can increase sensing accuracy [21] or frequency resolution [20]. Two-stage sensing can be described by different sensing PHY parameters for each stage. We denote the probability of detection as δ_a and δ_f , the probability of false alarm as ϕ_a

²We do not focus on recently proposed spectrum sensing methods for OFDMA networks, like [19] where quite-active sensing is proposed with non-active users sensing while others actively communicating, since they belong to a single-stage spectrum sensing category.

and ϕ_f , and the sensing time as τ_a and τ_f for coarse and fine sensing stages, respectively. When setting $\delta_a = 1$, $\phi_a = 1$ and $\tau_a = 0$ the two-stage sensing model reduces to a single stage sensing model.

In order to evaluate the effect of spectrum sensing on the system throughput, we need to determine the sensing strategy which determines when and how to switch to fine sensing from coarse sensing. Firstly, we consider a sensing strategy where the SU senses all channels, including the operating channel, with coarse sensing and when the SU detects the PU on any of the channels, it immediately switches to fine sensing. With this sensing strategy, if the transition between coarse and fine sensing does not occur frequently, sensing time can be reduced, which in-turn may increase the system throughput. We name this strategy as general two-stage sensing and denote it as S_0 .

Secondly, for a specific case when the bandwidth to transmit data is fixed and less than the whole allowed bandwidth, we investigate the following strategy. During coarse sensing the SU senses not the whole bandwidth but only a fixed bandwidth that is currently utilized for data transmission. If the PU is detected on the channel, the SU immediately senses all channels allowed to be utilized for the OSA system with fine sensing and switches to the channels detected as idle. We name this strategy as two-stage active channel sensing and denote it as S_1 . Since in this strategy there is no need to always sense all channels, the sensing time is reduced.

2) *Data PHY and MAC Layer:* Even though the OSA network is aware of subchannels being idle or busy, it should determine how to utilize the subchannels detected as idle for data transmission. There are numerous methods to utilize the idle subchannels in an OSA context, for a good overview we refer to [16]. However, we selectively study four strategies that are proper for the centrally-controlled OS-OFDMA-based network. Those four strategies can be classified into two groups based on the purpose of the strategies.

Firstly, we need a strategy to avoid utilizing the subchannels on which the PU is detected. An efficient strategy is to notch out the subchannel detected as busy and utilize all other available subchannels for OS-OFDMA. Note that we assume for simplicity that it is possible to notch out subchannels and transmit on the adjacent subchannels without causing interference³. We name this strategy subchannel notching and denote it as N_1 . On the opposite side, a conservative strategy is to exclude (block) the whole channel from accessing, even though only one subchannel is utilized by the PU, which is suggested for IEEE

³Refer to a recent studies on that topic that prove the feasibility of such approach. In [22] a sidelobe suppression with guard band equal to only one OFDM subcarrier interval was shown. In [23] a OFDM subcarrier notching was proposed with only 4% of the available spectrum wastage. Finally a practical implementation of OFDM subcarrier suppression with perfect channel utilization at the cost of throughput reduction was demonstrated in [24].

TABLE II
SUMMARY OF DESIGN OPTIONS OF CONSIDERED IN THE PAPER

Symbol	Two-Stage Sensing	Notching/Blocking	Bonding/Separation
$S_0N_1B_1$	General	Subchannel Notching	Subchannel Bonding
$S_0N_0B_1$	General	Channel Blocking	Channel Bonding
$S_0N_0B_0$	General	Channel Blocking	Fixed Channel Selection
$S_1N_0B_0$	Active Channel	Channel Blocking	Fixed Channel Selection

P802.22. However, this strategy does not maximize the efficiency because it wastes available OFDMA resources. We name this strategy channel blocking and denote it symbolically as N_0 .

Secondly, we also need to determine how much bandwidth is utilized for data transmission from the channels detected as idle. One strategy is to utilize all channels detected as idle from the allowed bandwidth. This strategy may maximize channel utilization for a given allowed bandwidth at the cost of the wideband RF and signal processing. We name this strategy as variable channel/subchannel bonding and denote it as B_1 . On the other hand, another strategy is to transmit data through only one channel selectively, even though there may exist more channels detected as idle. Because the SU operates on the bandwidth of only one channel, the cost for the RF and signal processing is low. However, it is inefficient because some available bandwidth may not be utilized. Since it is one of the operating modes of IEEE P802.22 we also include it in our study. We name this strategy fixed channel selection and denote it symbolically as B_0 .

3) *Design Options of Interest:* Because we have three groups of binary choices, i.e. S_x , N_x , and B_x , where $x \in \{0, 1\}$, there can be eight possible combinations of design options. However, not all options are feasible. First, we do not consider the combination of subchannel notching (N_1) and fixed channel selection (B_0), since it is a special case of N_1B_1 configuration with a single channel. Also, for two-stage active channel sensing (S_1), we only consider channel blocking (N_0) and fixed channel selection (B_0), because two-stage active channel sensing (S_1) is applicable to fixed bandwidth utilization case only. This leaves four combinations of the design options which are summarized in Table II.

III. ANALYSIS

A. Case $S_0N_1B_1$

Generally, in OFDMA-based wireless networks throughput depends on how many subchannels are utilized by CBR and VBR connections in the idle spectrum [15, Sec. III-B]. Let $\Pr_1(m_c, m_v, M_a)$ be

the probability that m_c and m_v number of subchannels are utilized by CBR and VBR connections, respectively⁴ when M_a number of subchannels are detected as idle. In addition, let $\eta(M_a)$ be the average ratio of data transmission time to total frame length when M_a number of subchannels are detected as idle. Then, the total system throughput H can be calculated as

$$H \triangleq C \sum_{M_a=0}^M \eta(M_a) \sum_{m_c, m_v \in \mathcal{Y}} (m_c + m_v) \Pr_1(m_c, m_v, M_a), \quad (1)$$

where $\mathcal{Y} = \{0, \dots, M\}$. The throughput of CBR, H_c , and VBR, H_v , is computed using (1) by replacing $m_c + m_v$ with m_c for H_c and m_v for H_v . The value of $\eta(\cdot)$ depends on the sensing stage since a longer sensing time for one stage can reduce $\eta(\cdot)$, while a shorter sensing time for another stage can increase $\eta(\cdot)$.

We introduce a variable S which indicates the sensing stage, such that $S = 0$ denotes the case when the OSA network performs only coarse sensing without switching to fine sensing, and $S > 0$ denotes the case when the OSA network performs coarse sensing and switches to fine sensing immediately. Specifically, $S = 1$ denotes the case when the OSA network detects the idle subchannel and $S = 2$ denotes the case that no idle subchannel is detected so that the network waits until the next sensing period without transmitting data. Defining $\Pr_0(S, M_a)$ as the joint probability that the current sensing stage equals to S and the number of subchannels detected as idle is M_a , we can compute η as

$$\eta(M_a) \triangleq \Pr_0(0, M_a) \frac{t_f - \tau_a}{t_f} + \Pr_0(1, M_a) \frac{t_f - \tau_a + \tau_f}{t_f}. \quad (2)$$

Note that there is no $\Pr_S(2, M_a)$ in (2) because for $S = 2$ no data can be transmitted, so the ratio of the data transmission time to the total frame length is zero. The probability $\Pr_0(\cdot)$ is given as (21) and will be derived later in this section.

To obtain H , H_c , and H_v we need to decompose $\Pr_1(\cdot)$ into conditions that describe the relation between different network functionalities and users. Values of m_c and m_v are easily determined if we know the number of CBR connections connected with the BS, U_c , the number of VBR connections connected with the BS, U_v , and the number of subchannels detected as idle, M_a . Thus

$$\Pr_1(\cdot) \triangleq \sum_{U_c=0}^{U_{c,\max}} \sum_{U_v=0}^{U_{v,\max}} \Pr_2(m_c, m_v | U_c, U_v, M_a) \Pr_3(U_c, U_v, M_a). \quad (3)$$

To derive $\Pr_2(\cdot)$ used in (3) we observe that the total number of subchannels used by all CBR users, $U_c l_c$, cannot be greater than the number of the available subchannels, M_a , because if there is no subchannel

⁴In the paper we follow the convention that each newly introduced probability will be uniquely identified by a number and introduced with all argument variables, while its later callouts will be referred as $\Pr_x(\cdot)$.

available the CBR connection will be blocked. Thus we only consider the case when $U_c l_c \leq M_a$. Since a CBR connection has a higher priority than a VBR connection, all CBR connections can transmit data through all $m_c = U_c l_c$ subchannels. Then the remaining subchannels, i.e. $m_v = M_a - U_c l_c$, are used by VBR connections. On the other hand, if there are no VBR connections in the system, $m_v = 0$. Therefore, defining $f_+(x)$, where $f_+(0) = 0$ and $f_+(x > 0) = 1$ we have

$$\Pr_2(\cdot) \triangleq \begin{cases} 1, & U_c l_c \leq M_a, m_c = U_c l_c, m_v = (M_a - U_c l_c) f_+(U_v); \\ 0, & \text{otherwise.} \end{cases} \quad (4)$$

To calculate $\Pr_3(\cdot)$ in (3), we model SU traffic as a Markov chain with the state $\{U_c, U_v, M_a\}$. Using the state transition probability $\Pr_4(U_c^{(t)}, U_v^{(t)}, M_a^{(t)} | U_c^{(t-1)}, U_v^{(t-1)}, M_a^{(t-1)})$ which describes the change in U_c, U_v, M_a between time $t-1$ and t , we can compute $\Pr_3(\cdot)$ by solving the Markov chain, given $\sum_{\mathcal{M}} \Pr_3(\cdot) = 1$ and $\Pr_3(\cdot) = \sum_{\mathcal{M}^{(t-1)}} \Pr_3(\cdot) \Pr_4(\cdot)$, where \mathcal{M} is a set of possible states $\{U_c, U_v, M_a\}$ and $\mathcal{M}^{(t-1)}$ is a set of the states at time $t-1$. Based on the conditional probability property and independency of the variables, we decompose $\Pr_4(\cdot)$ as

$$\Pr_4(\cdot) \triangleq \Pr_5(U_c^{(t)}, U_v^{(t)} | U_c^{(t-1)}, U_v^{(t-1)}, M_a^{(t)}, M_a^{(t-1)}) \Pr_6(M_a^{(t)} | M_a^{(t-1)}). \quad (5)$$

First we derive $\Pr_5(\cdot)$ in (5). Recall that we assume that the CBR has higher priority than the VBR, and thus the VBR utilizes the remaining subchannels after subchannel assignment for all CBRs. Then, defining $\Pr_7(U_c^{(t)} | U_c^{(t-1)}, M_a^{(t)}, M_a^{(t-1)})$ as the conditional probability of the number of the CBRs at time t for the given number of subchannels detected as idle, and $\Pr_8(U_v^{(t)} | U_v^{(t-1)}, U_c^{(t)}, U_c^{(t-1)}, M_a^{(t)}, M_a^{(t-1)})$ as the conditional probability of the number of VBR users at time t for the given number of CBR users and the available subchannels, we have

$$\Pr_5(\cdot) \triangleq \Pr_8(U_v^{(t)} | U_v^{(t-1)}, U_c^{(t)}, U_c^{(t-1)}, M_a^{(t)}, M_a^{(t-1)}) \Pr_7(U_c^{(t)} | U_c^{(t-1)}, M_a^{(t)}, M_a^{(t-1)}). \quad (6)$$

To derive $\Pr_7(\cdot)$ and $\Pr_8(\cdot)$ in (6), we introduce functions $G_x(i | U_x)$ and $T_x(j | \mu_x)$ with supporting variables i and j denoting $G_x(i | U_x)$ as the probability that i connections are newly generated from U_x users, and $T_x(j | \mu_x)$ as the probability that j connections are released with departure rate μ_x . $G_x(i | U_x)$ and $T_x(j | \mu_x)$ are derived in Appendix A. Our approach to derive $\Pr_7(\cdot)$ and $\Pr_8(\cdot)$ is to calculate all possible sets for i and j and apply them to $G_x(i | U_x)$ and $T_x(j | \mu_x)$.

First, we consider valid conditions for $U_c^{(t)}, U_c^{(t-1)}, M_a^{(t)}$, and $M_a^{(t-1)}$ to derive $\Pr_7(\cdot)$. We denote the number of users being able to utilize all available subchannels as $U_a^{(t)} = \lfloor M_a^{(t)} / l_c \rfloor$ at time t and $U_a^{(t-1)} = \lfloor M_a^{(t-1)} / l_c \rfloor$ at time $t-1$. Then, because $U_a^{(t-1)}, U_a^{(t)}$ denote the maximum number of users

$U_c^{(t)} \leq U_a^{(t)}$ and $U_c^{(t-1)} \leq U_a^{(t-1)}$. Next, because the possible sets of i and j are different for the cases $U_c^{(t)} < U_a^{(t)}$, $U_c^{(t)} = U_a^{(t)} > 0$, and $U_c^{(t)} = U_a^{(t)} = 0$, we consider them separately.

The first case, $U_c^{(t)} < U_a^{(t)}$, represents the situation when the number of subchannels detected as idle is more than the number of all subchannels that will be utilized by CBR connections before spectrum sensing. In other words, no CBR connection is blocked due to the PU appearance. Because the number of CBR connections is $U_c^{(t-1)}$ at time $t-1$ and $U_c^{(t)}$ at time t , the change in the number of CBR connections is $i - j = U_c^{(t)} - U_c^{(t-1)}$. In addition, because there are $U_c^{(t-1)}$ active connections at time $t-1$, more than $U_c^{(t-1)}$ connections cannot be released, i.e. $j \leq U_c^{(t-1)}$. Therefore $\{i, j\} \in \mathcal{K}_{c,a} \triangleq \{i, j | i - j = U_c^{(t)} - U_c^{(t-1)}, j \leq U_c^{(t-1)}\}$.

The second case, $U_c^{(t)} = U_a^{(t)} > 0$, denotes the situation when CBR connections may be blocked due to the PU arrival. Then, before spectrum sensing, the total number of connections including newly generated connections is $U_c^{(t-1)} + i - j$. However, after spectrum sensing, the connections that utilize subchannels detected as busy are blocked and the remaining connections, $U_c^{(t)}$, utilize all available subchannels, $M_a^{(t)}$. Thus, the number of CBR connections before spectrum sensing, $U_c^{(t-1)} + i - j$, can be greater than or equal to the number of CBR connections after spectrum sensing, $U_c^{(t)}$, but should be less than or equal to $U_{c,\max}$, i.e. $U_c^{(t)} \leq U_c^{(t-1)} + i - j \leq U_{c,\max}$. Therefore $\{i, j\} \in \mathcal{K}_{c,b} \triangleq \{i, j | U_c^{(t)} - U_c^{(t-1)} \leq i - j \leq U_{c,\max} - U_c^{(t-1)}, j \leq U_c^{(t-1)}\}$.

The third and final case is when $U_a^{(t)} = U_c^{(t)} = 0$. In this situation, because there is no subchannels available for CBR, the number of CBR connections should also be zero. Consequently, regardless of i and j , the conditional probability $\text{Pr}_7(\cdot)$ under this condition is always one. Considering all possible cases, $\text{Pr}_7(\cdot)$ is derived as

$$\text{Pr}_7(\cdot) \triangleq \begin{cases} \sum_{\{i,j\} \in \mathcal{K}_{c,a}} T_c(j|\mu_c) G_c(i|U_c^{(t-1)}), & U_c^{(t-1)} \leq U_a^{(t-1)}, U_c^{(t)} < U_a^{(t)}; \\ \sum_{\{i,j\} \in \mathcal{K}_{c,b}} T_c(j|\mu_c) G_c(i|U_c^{(t-1)} + i - j), & U_c^{(t-1)} \leq U_a^{(t-1)}, U_c^{(t)} = U_a^{(t)} > 0; \\ 1, & U_c^{(t-1)} \leq U_a^{(t-1)}, U_c^{(t)} = U_a^{(t)} = 0. \end{cases} \quad (7)$$

For VBR traffic, assuming all VBR connections share the same portion of the idle bandwidth, we calculate the number of subchannels for one VBR connection, l_v , as

$$l_v = \begin{cases} \frac{M_a^{(t-1)} - U_c^{(t-1)}}{U_v^{(t-1)}}, & U_v^{(t-1)} > 0, \\ 0, & U_v^{(t-1)} = 0. \end{cases} \quad (8)$$

Furthermore, we do not need to consider the case that the VBR connection is blocked by the PU because VBR connections are assumed to be buffered instead of blocked when there is no available subchannel.

Thus, with the l_v subchannels, $\text{Pr}_8(\cdot)$ from (6) is defined as

$$\text{Pr}_8(\cdot) \triangleq \sum_{\{i,j\} \in \mathcal{K}_v} T_v(j|l_v \mu_v) G_v(i|U_v^{(t)}), \quad (9)$$

where $\mathcal{K}_v \triangleq \{i, j | i - j = U_v^{(t)} - U_v^{(t-1)}, j \leq U_v^{(t-1)}\}$. Finally, substituting (7) and (9) into (6), we obtain $\text{Pr}_5(\cdot)$.

We can now derive the state transition probability of the subchannels detected as idle, $\text{Pr}_6(\cdot)$ in (5). This probability is defined as

$$\text{Pr}_6(\cdot) \triangleq \frac{\text{Pr}_9(M_a^{(t)}, M_a^{(t-1)})}{\text{Pr}_{10}(M_a^{(t-1)})}. \quad (10)$$

We need to define $\text{Pr}_9(\cdot)$ and $\text{Pr}_{10}(\cdot)$ in (10). We start with the definition of $\text{Pr}_9(\cdot)$, denoting $\text{Pr}_{11}(M_a^{(t)}, M_a^{(t-1)} | U_w^{(t)}, U_n^{(t)}, S^{(t)})$ as the conditional probability of the number of subchannels detected as idle given the numbers of WPUs and NPU's and the sensing stage, and $\text{Pr}_{12}(U_w^{(t)}, U_w^{(t-1)}, U_n^{(t)}, U_n^{(t-1)}, S^{(t)}, S^{(t-1)})$ as the joint probability of the numbers of WPUs and NPU's and the sensing stage, as

$$\begin{aligned} \text{Pr}_9(\cdot) \triangleq & \sum_{\forall U_w^{(t)}, U_n^{(t)}, S^{(t)}, U_w^{(t-1)}, U_n^{(t-1)}, S^{(t-1)}} \text{Pr}_{12}(U_w^{(t)}, U_w^{(t-1)}, U_n^{(t)}, U_n^{(t-1)}, S^{(t)}, S^{(t-1)}) \\ & \times \text{Pr}_{11}(M_a^{(t)}, M_a^{(t-1)} | U_w^{(t)}, U_w^{(t-1)}, U_n^{(t)}, U_n^{(t-1)}, S^{(t)}, S^{(t-1)}), \end{aligned} \quad (11)$$

where $S^{(t)}$ and $S^{(t-1)}$ are the sensing stages at times t and $t-1$, respectively.

Probability $\text{Pr}_{11}(\cdot)$ in (11) can be decomposed into products of probabilities at time t and time $t-1$, because the number of subchannels detected as idle and the state of the sensing stage at time slot t is independent from time $t-1$. That is

$$\text{Pr}_{11}(\cdot) \triangleq \text{Pr}_{13}(M_a^{(t-1)} | U_w^{(t-1)}, U_n^{(t-1)}, S^{(t-1)}) \text{Pr}_{13}(M_a^{(t)} | U_w^{(t)}, U_n^{(t)}, S^{(t)}). \quad (12)$$

In $\text{Pr}_{13}(\cdot)$ in (12), M_a subchannels include M_m subchannels that are occupied by PUs but mis-detected and M_0 subchannels correctly detected as idle. Therefore, $M_a = M_m + M_0$, and thus to compute $\text{Pr}_{13}(\cdot)$ we define a supporting probability, $\text{Pr}_{14}(M_m, M_0 | U_w, U_n, S)$, which is the probability that the number of subchannels detected as idle correctly and falsely are M_0 and M_m , respectively.

In design option S_0 , a SU performs the coarse sensing for all subchannels first, and then, if the SU detects a PU on a subchannel, it immediately switches to fine sensing and senses all subchannels again with high sensing accuracy. Thus, for a condition $S = 0$ (only coarse sensing is performed), the number of subchannels detected as idle must be the same as the number of all subchannels, i.e. $M_m + M_0 = M$. In other words, the case $M_m + M_0 < M$ is impossible for the condition $S = 0$. For the condition $S = 2$

(no idle subchannel is detected after all stages of sensing) only the case $M_m + M_0 = 0$ is possible. For $S = 1$, using the detection probability δ_f and the false alarm probability ϕ_f in the fine sensing stage, we can derive the probability that M_m busy subchannels are mis-detected and M_0 idle subchannels are correctly detected for given U_w WPU and U_n NPU. Thus,

$$\Pr_{14}(\cdot) \triangleq \begin{cases} F & S = 1; \\ 1, & S = 0, M_m + M_0 = M, \text{ or } S = 2, M_m + M_0 = 0; \\ 0, & S = 0, M_m + M_0 < M, \text{ or } S = 2, M_m + M_0 > 0, \end{cases} \quad (13)$$

where $F = \binom{M_p}{M_m} (1 - \delta_f)^{M_m} \delta_f^{M_p - M_m} \binom{M - M_p}{M_0} (1 - \phi_f)^{M_0} \phi_f^{M - M_p - M_0}$, and $M_p = \min(M, U_w l_w + U_n l_n)$ is the number of subchannels actually occupied by PUs. Therefore, $\Pr_{13}(\cdot)$ in (12) can be derived as

$$\Pr_{13}(\cdot) \triangleq \sum_{x=0}^{M_a} \Pr_{14}(x, M_a - x | U_w, U_n, S). \quad (14)$$

Probability $\Pr_{12}(\cdot)$ in (11) can then be decomposed into conditional probabilities as follows

$$\begin{aligned} \Pr_{12}(\cdot) &\triangleq \Pr_{15} \left(S^{(t)} | U_w^{(t)}, U_n^{(t)} \right) \Pr_{15} \left(S^{(t-1)} | U_w^{(t-1)}, U_n^{(t-1)} \right) \\ &\quad \times \Pr_{16} \left(U_w^{(t)}, U_n^{(t)} | U_w^{(t-1)}, U_n^{(t-1)} \right) \Pr_{17} \left(U_w^{(t-1)}, U_n^{(t-1)} \right), \end{aligned} \quad (15)$$

where $\Pr_{16}(\cdot)$ and $\Pr_{17}(\cdot)$ are the state transition probability and the steady state probability for the state $\{U_w, U_n\}$, respectively, and $\Pr_{15}(\cdot)$ is the conditional probability of the sensing stage given the number of NPUs and WPUs.

To derive $\Pr_{15}(\cdot)$ we need to consider the following three cases. First, if the OSA network mis-detects existing PUs and correctly detects all idle subchannels in the coarse sensing stage, $S = 0$ because OSA network will not advance to fine sensing. Second, if the OSA network detects at least one PU correctly or falsely in the coarse sensing stage and detects all subchannels as busy also correctly or falsely in the fine sensing stage, $S = 2$ because after coarse and fine sensing no idle subchannel is detected. Otherwise $S = 1$. Thus,

$$\Pr_{15}(\cdot) \triangleq \begin{cases} (1 - \delta_a)^{M_p} (1 - \phi_a)^{M - M_p}, & S = 1; \\ (1 - (1 - \delta_a)^{M_p} (1 - \phi_a)^{M - M_p}) \delta_f^{M_p} \phi_f^{M - M_p}, & S = 3; \\ 1 - \Pr_{15}(S = 1 | U_w, U_n) - \Pr_{15}(S = 3 | U_w, U_n), & S = 2. \end{cases} \quad (16)$$

Next, we can compute probability $\Pr_{17}(\cdot)$ in (15) by solving a Markov chain with a state $\{U_w, U_n\}$, such that $\sum_{\mathcal{U}} \Pr_{17}(\cdot) = 1$ and $\Pr_{17}(\cdot) = \sum_{\mathcal{U}^{(t-1)}} \Pr_{17}(\cdot) \Pr_{16}(\cdot)$, where \mathcal{U} is the set of all possible values of U_w and U_n and $\mathcal{U}^{(t-1)}$ is the set of the same parameters at time $t - 1$. Based on the assumption that

the WPU has a higher priority of channel access than the NPU, the state transition probability $\text{Pr}_{16}(\cdot)$ is derived as

$$\text{Pr}_{16}(\cdot) \triangleq \text{Pr}_{18}\left(U_w^{(t)}|U_w^{(t-1)}\right) \text{Pr}_{19}\left(U_n^{(t)}|U_n^{(t-1)}, U_w^{(t)}, U_w^{(t-1)}\right). \quad (17)$$

Because we assume that the inter-arrival time and departure time follows the negative exponential distribution, we can use equations (41) and (42), derived in Appendix A, in the similar way as in the derivation of (7) and (9). By denoting the available subchannels for NPU as $U_{e2} = \lfloor (M - U_w^{(t)} l_w) / l_n \rfloor$ at time t and $U_{e1} = \lfloor (M - U_w^{(t-1)} l_w) / l_n \rfloor$ at time $t-1$, we can derive $\text{Pr}_{18}(\cdot)$ and $\text{Pr}_{19}(\cdot)$ as

$$\text{Pr}_{18}(\cdot) \triangleq \sum_{\{i,j\} \in \mathcal{K}_w} G_w(i|U_w^{(t)}) T_w(j|\mu_w), \quad (18)$$

$$\text{Pr}_{19}(\cdot) \triangleq \begin{cases} \sum_{\{i,j\} \in \mathcal{K}_{n,a}} T_n(j|\mu_n) G_n(i|U_n^{(t)}), & U_n^{(t-1)} \leq U_{e1}, U_n^{(t)} < U_{e2}; \\ \sum_{\{i,j\} \in \mathcal{K}_{n,b}} T_n(j|\mu_n) G_n(i|U_n^{(t-1)} + i - j), & U_n^{(t-1)} \leq U_{e1}, U_n^{(t)} = U_{e2}, \end{cases} \quad (19)$$

where $\mathcal{K}_w \triangleq \{i, j | i - j = U_w^{(t)} - U_w^{(t-1)}, j \leq U_w^{(t-1)}\}$, $\mathcal{K}_{n,a} \triangleq \{i, j | i - j = U_n^{(t)} - U_n^{(t-1)}, j \leq U_n^{(t-1)}\}$ and $\mathcal{K}_{n,b} \triangleq \{i, j | U_n^{(t)} - U_n^{(t-1)} \leq i - j \leq U_{n,\max} - U_n^{(t-1)}, j \leq U_n^{(t-1)}\}$.

Now $\text{Pr}_{10}(\cdot)$ in (10) is calculated as

$$\text{Pr}_{10}(\cdot) \triangleq \sum_{\forall U_w, U_n, S} \text{Pr}_{13}(M_a|U_w, U_n, S) \text{Pr}_{15}(S|U_w, U_n) \text{Pr}_{17}(U_w, U_n). \quad (20)$$

Finally, by taking out a summation parameter S in (20), we can derive $\text{Pr}_0(\cdot)$ in (2) as

$$\text{Pr}_0(\cdot) \triangleq \sum_{\forall U_w, U_n} \text{Pr}_{13}(M_a|U_w, U_n, S) \text{Pr}_{15}(S|U_w, U_n) \text{Pr}_{17}(U_w, U_n). \quad (21)$$

B. Case $S_0 N_0 B_1$

There are two major changes for the analysis of $S_0 N_0 B_1$ case in comparison to $S_0 N_1 B_1$. First, the number of subchannels detected as idle should be the integer multiples of Y because in this case the smallest quantity of idle bandwidth is one channel. Second, the number of available subchannels is determined not only by the number of the NPUs but also by the position of the NPUs in the spectrum. For example, if two NPUs appear on different subchannels in the same channel, the SU cannot utilize that channel. While if NPUs occupy subchannels located in two different channels, those two channels cannot be used by SUs. Considering those changes, we need to modify probabilities related to the number of subchannels detected as idle and the sensing stage used, that is $\text{Pr}_{13}(\cdot)$ in (14), $\text{Pr}_{11}(\cdot)$ in (12) and $\text{Pr}_{15}(\cdot)$ in (16). Note that the other probabilities remain the same as derived in Section III-A. For the following analysis we assume $\delta_f \cong \delta_a \cong 1$ to reduce the complexity of calculation. In general, the

OS-OFDMA system needs to keep a high detection probability to protect the PUs, which makes this approximation reasonable. Note that we will still consider the effect of false alarms. Thus, even if there is no PU on the spectrum, the SU may falsely detect an idle subchannel as busy. Moreover, without loss of generality, we assume that a WPU occupies one channel, i.e., $l_w = Y$.

First, we modify $\text{Pr}_{13}(\cdot)$, the probability of the number of subchannels detected as idle for a given number of WPUs and NPUs and the sensing stage. For the case $S_0N_0B_1$, because the spectrum is utilized based on the unit of bandwidth of one channel rather than one subchannel, we introduce the probability of the number of channels detected as idle, X_a , to compute the probability of the number of subchannels detected as idle, M_a . Denoting $\text{Pr}_{20}(X_a|U_w, U_n, S)$ as the probability that the number of channels detected as idle is X_a given U_w WPUs and U_n NPUs in the S sensing stage, (14) is modified as

$$\text{Pr}_{13}(\cdot) \triangleq \begin{cases} \text{Pr}_{20}(X_a|U_w, U_n, S), & M_a = X_a Y, \\ 0, & \text{otherwise.} \end{cases} \quad (22)$$

There are two required conditions for $\text{Pr}_{20}(\cdot)$ in (22). First, the sum of the channels detected as idle and the number of WPUs cannot be greater than the total number of channels, i.e. $X_a + U_w \leq X$. Second, the number of NPUs cannot be greater than the total number of subchannels that are not occupied by the WPUs, i.e. $U_n \leq (X - U_w)\lfloor Y/l_n \rfloor$. We denote $\mathbf{1}_c$ as an indicator of those conditions, defining $\mathbf{1}_c = 1$ for $X_a + U_t \leq X$ or $U_n \leq (X - U_w)\lfloor Y/l_n \rfloor$ and $\mathbf{1}_c = 0$, otherwise.

Next, we compute $\text{Pr}_{20}(\cdot)$ under the feasible conditions considering different sensing stages. Under the condition that no channel is detected as idle after the fine sensing, i.e. $S = 2$, the number of channels detected as idle is $X_a = 0$ under the assumption of perfect PU detection. On the other hand, when all channels are detected as idle in the coarse sensing, i.e. $S = 0$, only $X_a = X$ is possible. The analysis for the condition that the SU performs fine sensing and detects idle channels, i.e. $S = 1$, is not easy to derive directly because the number of channels detected as idle depends on the position of NPUs in the spectrum as well as the number of NPUs. Thus, defining the number of channels actually occupied by the NPU as X_n , we deconstruct $\text{Pr}_{20}(\cdot)$ for $S = 1$ into two components: the conditional probability of X_n for given number of PUs and the sensing stage, denoted as $\text{Pr}_{21}(X_n|U_w, U_n, S)$, and the conditional probability

of the number of channels detected as idle for a given X_n , denoted as $\text{Pr}_{22}(X_a|X_n, U_w, U_n, S)$. Then,

$$\text{Pr}_{20}(\cdot) \triangleq \begin{cases} \sum_{\mathcal{X}} \text{Pr}_{21}(X_n|U_w, U_n, S) \text{Pr}_{22}(X_a|X_n, U_w, U_n, S), & \mathbf{1}_c = 1, S = 2; \\ & \mathbf{1}_c = 1 \text{ and } S = 0, \\ & X_a = X \text{ or } S = 2, \\ & X_a = 0; \\ 1, & \text{otherwise,} \\ 0, & \end{cases} \quad (23)$$

where $\mathcal{X} = \{X_n | \lceil (U_n l_n / Y) \rceil \leq X_n \leq \min(U_n, X - U_t - X_a)\}$ because X_n is the smallest when all NPUs are located on adjacent subchannels, i.e. $\lceil (U_n l_n) / Y \rceil$, and the largest when all NPUs are located in different channels separated as far as possible, i.e. $\min(U_n, X - U_t - X_a)$.

To compute $\text{Pr}_{21}(\cdot)$ in (23), we assume that any NPU can appear on any subchannel with equal probability, and that false alarm can occur uniformly over all idle subchannels. Then, we introduce a supporting function $f_s(k, x, r)$ denoting the number of possibilities that k items are distributed over exactly x bins each of which has a capacity of r items (see Appendix B for the derivation). Then $\text{Pr}_{21}(\cdot)$ can be computed by dividing the number of possible events that U_n NPUs are located on exactly X_n channels each of which can have at maximum $\lfloor Y/l_n \rfloor$ NPUs, i.e. $f_s(U_n, X_n, \lfloor Y/l_n \rfloor)$, by the number of all possible events that U_n NPUs appear on $X - U_w$ channels, i.e. $\binom{X - U_w}{U_n}^{\lfloor Y/l_n \rfloor}$. Note that if there is no NPU, i.e. $U_n = 0$, then X_n should be zero. Considering the possible case of selecting X_n NPU channels from a total of $X - U_w$ channels, i.e. $\binom{X - U_w}{X_n}$, we derive $\text{Pr}_{21}(\cdot)$ as

$$\text{Pr}_{21}(\cdot) = \begin{cases} 1, & X_n = 0, U_n = 0, \\ \frac{\binom{X - U_w}{X_n} f_s(U_n, X_n, \lfloor Y/l_n \rfloor)}{\binom{X - U_w}{U_n}^{\lfloor Y/l_n \rfloor}}, & \text{otherwise.} \end{cases} \quad (24)$$

Now we present the derivation of $\text{Pr}_{22}(\cdot)$ in (23). If there exist U_w and X_n channels that are occupied by WPU and NPUs, respectively, and X_a channels are correctly detected as idle, the remaining $X - U_w - X_n - X_a$ channels must be falsely detected as busy. Considering the number of events of selecting X_a channels from $X - U_w - X_n$ idle channels, we derive $\text{Pr}_{22}(\cdot)$ as

$$\text{Pr}_{22}(\cdot) = \binom{X - U_w - X_n}{X_a} (1 - (1 - \phi_f)^Y)^{X - U_w - X_n - X_a} (1 - \phi_f)^{Y X_a}. \quad (25)$$

Next, we modify $\text{Pr}_{11}(\cdot)$ from (12). The change of the number of PUs between time t and $t - 1$ may affect the change of the position of the PUs and, as a result, can make an impact on the number of channels detected as idle at time t . Thus, introducing the conditional probability of the number of

idle subchannels as $\Pr_{23} \left(M_a^{(t)} | U_w^{(t)}, U_n^{(t)}, S^{(t)}, M_a^{(t-1)}, U_w^{(t-1)}, U_n^{(t-1)}, S^{(t-1)} \right)$, $\Pr_{11}(\cdot)$ in (12) is newly defined as

$$\begin{aligned} \Pr_{11}(\cdot) &\triangleq \Pr_{13} \left(M_a^{(t-1)} | U_w^{(t-1)}, U_n^{(t-1)}, S^{(t-1)} \right) \\ &\times \Pr_{23} \left(M_a^{(t)} | M_a^{(t-1)}, U_w^{(t)}, U_w^{(t-1)}, U_n^{(t)}, U_n^{(t-1)}, S^{(t)}, S^{(t-1)} \right). \end{aligned} \quad (26)$$

Again, because for $S_0N_0B_1$ the spectrum is utilized based on the unit of bandwidth of one channel, denoting $\Pr_{24} \left(X_a^{(t)} | X_a^{(t-1)}, U_w^{(t)}, U_w^{(t-1)}, U_n^{(t)}, U_n^{(t-1)}, S^{(t)}, S^{(t-1)} \right)$ as the conditional probability of the number of channels, we derive $\Pr_{23}(\cdot)$ as follows

$$\Pr_{23}(\cdot) \triangleq \begin{cases} \Pr_{24}(X_a^{(t)} | X_a^{(t-1)}, U_w^{(t)}, U_w^{(t-1)}, U_n^{(t)}, U_n^{(t-1)}, S^{(t)}, S^{(t-1)}), & M_a = X_a Y, \\ 0, & \text{otherwise.} \end{cases} \quad (27)$$

To reduce the complexity of calculating $\Pr_{24}(\cdot)$ we use an approximation that if the number of PUs is the same at times t and $t-1$, the positions of NPUs at times t and $t-1$ are also the same. This approximation is valid when the PU activity is not high. With this approximation we ignore the case that a certain number of NPUs disappear while at the same time the same number of new NPUs appear, but at different locations. Also we assume that if the number of WPU and NPUs have changed, the number of channels detected as idle is independent of the number of WPU and NPUs at time $t-1$, which means that $\Pr_{24}(\cdot) \cong \Pr_{20}(\cdot)$. Considering these approximations we derive $\Pr_{24}(\cdot)$ as

$$\Pr_{24}(\cdot) \cong \begin{cases} 1, & U_w^{(t)} = U_w^{(t-1)}, U_n^{(t)} = U_n^{(t-1)}, X_a^{(t)} = X_a^{(t-1)}; \\ 0, & U_w^{(t)} = U_w^{(t-1)}, U_n^{(t)} = U_n^{(t-1)}, X_a^{(t)} \neq X_a^{(t-1)}; \\ \Pr_{20}(X_a | U_w, U_n, S), & \text{otherwise.} \end{cases} \quad (28)$$

Finally, we need to modify $\Pr_{15}(\cdot)$ in (16) under the approximation of the perfect detection. Depending on the number of subchannels occupied by PUs, i.e. M_p , we consider three cases. In the first case, $M_p = M$, all subchannels are occupied by PUs. Then, because of the perfect detection approximation $S = 2$ is the only feasible condition. In the second case, $M_p = 0$, no PU appears on the subchannels. In this case, the false alarm probability of each sensing stage affects the probability $\Pr_{15}(\cdot)$. In the last case, $0 < M_p < M$, the probability of $S = 0$ is zero and the false alarm probability of the coarse sensing

does not affect the performance. Thus

$$\Pr_{15}(\cdot) = \begin{cases} 1, & M_p = M, S = 2; \\ (1 - \phi_a)^M, & M_p = 0, S = 0; \\ 1 - (1 - \phi_a)^M - \phi_a^M (\phi_f)^M, & M_p = 0, S = 1; \\ \phi_a^M \phi_f^M, & M_p = 0, S = 2; \\ 1 - \phi_f^{M-M_p}, & 0 < M_p < M, S = 1; \\ \phi_f^{M-M_p}, & 0 < M_p < M, S = 2; \\ 0, & \text{otherwise.} \end{cases} \quad (29)$$

C. Case $S_0 N_0 B_0$

To implement channel bonding in OS-OFDMA a wideband RF circuit is needed, which may be expensive. To reduce the cost, only one channel may be used for data transmission from all channels detected as idle. Note that the analysis in this section is based on the derivation from Section III-B since this option still considers subchannel non-notching. The major change here is that we perform analysis for data transmission on one channel instead of all X channels. This change affects the valid condition for $\Pr_7(\cdot)$ in (7) and l_v in (8). Because the maximum number of subchannels available is limited to Y , $U_a^{(t)}$ and $U_a^{(t-1)}$ becomes $\left\lfloor \min \left(Y/l_n, M_a^{(t)}/l_n \right) \right\rfloor$ and $\left\lfloor \min \left(Y/l_n, M_a^{(t-1)}/l_n \right) \right\rfloor$, respectively. Moreover, considering that the maximum number of channels utilized by VBR is also limited to one channel, then (8) should be modified as

$$l_v = \begin{cases} \frac{\min(Y, M_a^{(t-1)}) - U_c^{(t-1)}}{U_v^{(t-1)}}, & U_v^{(t-1)} > 0, \\ 0, & U_v^{(t-1)} = 0. \end{cases} \quad (30)$$

Also, we need to modify $\Pr_6(\cdot)$ in (10) considering the limitations of the available subchannels. Even if a SU detects more than one idle channel, the SU will utilize only one channel. In terms of the definition, we have to sum all probabilities that the number of subchannels detected as idle is greater than or equal to Y , in order to compute the probability that one channel, i.e. Y subchannels, are detected as idle. Thus,

$$\Pr_6(\cdot) \triangleq \begin{cases} \frac{\Pr_9(0,0)}{\Pr_{10}(0)}, & M_a^{(t)} = 0, M_a^{(t-1)} = 0, \\ \frac{\sum_{x=Y}^M \Pr_9(0,x)}{\sum_{x=Y}^M \Pr_{10}(x)}, & M_a^{(t)} = 0, M_a^{(t-1)} > 0, \\ \frac{\sum_{x=Y}^M \Pr_9(x,0)}{\Pr_{10}(0)}, & M_a^{(t)} > 0, M_a^{(t-1)} = 0, \\ \frac{\sum_{x,y \in \mathcal{Z}} \Pr_9(x,y)}{\sum_{x=Y}^M \Pr_{10}(x)}, & M_a^{(t)} > 0, M_a^{(t-1)} > 0, \end{cases} \quad (31)$$

where $\mathcal{Z} = \{Y, \dots, M\}$. Note that according to (14) and (24), $\text{Pr}_9(\cdot)$ and $\text{Pr}_{10}(\cdot)$ can have values only if the number of subchannels detected as idle, $M_a^{(t)}$ and $M_a^{(t-1)}$, are multiples of Y .

D. Case $S_1N_0B_0$

In this case the SU performs the coarse sensing for only one channel currently utilized for data transmission. Thus, the PU on a channel not used by the SU does not affect the OSA network, and as a result, the sensing stage of the OSA network becomes more sensitive to the location of the PUs in the radio spectrum. Therefore, probabilities related to the sensing stage S , such as $\text{Pr}_{20}(\cdot)$ of (23) in Section III-B, and $\text{Pr}_{12}(\cdot)$ of (15) and $\text{Pr}_{15}(\cdot)$ of (16) in Section III-A, need to be updated.

First, we update the definition of $\text{Pr}_{20}(\cdot)$. In option $S_1N_0B_0$, even if more than one channel is detected as idle, only one channel is utilized for data transmission. Thus, we consider only the case when one channel was detected as idle even though there can be more channels detected as idle. Then, obviously if a OSA network detects the idle channel, i.e. $S < 2$, the number of channels detected as idle is one. If $S = 2$, the probability that no idle channel is detected is also one. Thus $\text{Pr}_{20}(\cdot)$ can be modified as

$$\text{Pr}_{20}(\cdot) \triangleq \begin{cases} 1, & X_a = 0, S = 2 \text{ or } X_a = 1, S < 2, \\ 0, & \text{otherwise.} \end{cases} \quad (32)$$

Next, we present the modification of $\text{Pr}_{12}(\cdot)$ in (15). This modification is based on the fact that the sensing stage at time t can be affected by the number and the position of WPUs and the NPU at time $t - 1$. Thus, denoting $\text{Pr}_{25}(S^{(t)}|U_w^{(t)}, U_n^{(t)}, S^{(t-1)}, U_w^{(t-1)}, U_n^{(t-1)})$ as the conditional probability of the sensing stage at time t given the number of NPUs and WPUs for times t and $t - 1$, $\text{Pr}_{12}(\cdot)$ is modified as follows

$$\begin{aligned} \text{Pr}_{12}(\cdot) &\triangleq \text{Pr}_{25}(S^{(t)}|U_w^{(t)}, U_n^{(t)}, S^{(t-1)}, U_w^{(t-1)}, U_n^{(t-1)}) \text{Pr}_{15}(S^{(t-1)}|U_w^{(t-1)}, U_n^{(t-1)}) \\ &\times \text{Pr}_{16}(U_w^{(t)}, U_n^{(t)}|U_w^{(t-1)}, U_n^{(t-1)}) \text{Pr}_{17}(U_w^{(t-1)}, U_n^{(t-1)}). \end{aligned} \quad (33)$$

For the same reason as in case of $\text{Pr}_{12}(\cdot)$, $\text{Pr}_{15}(\cdot)$ in (16) needs to be modified as well. Denoting $\text{Pr}_{26}(S, U_w, U_n)$ as the joint probability of the number of PUs and the sensing stage, we derive $\text{Pr}_{15}(\cdot)$ as

$$\text{Pr}_{15}(\cdot) \triangleq \frac{\text{Pr}_{26}(S, U_w, U_n)}{\text{Pr}_{17}(U_w, U_n)}. \quad (34)$$

Because expression $\text{Pr}_{26}(\cdot)$ is the steady state probability, denoting the state transition probability as $\text{Pr}_{27}(S^{(t)}, U_w^{(t)}, U_n^{(t)}|S^{(t-1)}, U_w^{(t-1)}, U_n^{(t-1)})$, $\text{Pr}_{26}(\cdot)$ can be obtained by solving the Markov chain with a state $\{S, U_w, U_n\}$, such that $\text{Pr}_{26}(\cdot) = \sum_{S^{(t-1)}} \text{Pr}_{26}(\cdot) \text{Pr}_{27}(\cdot)$ and $\sum_S \text{Pr}_{26}(\cdot) = 1$, where S is the set

of all possible S , U_w , and U_n , and $\mathcal{S}^{(t-1)}$ is the set of the same variables at time $t - 1$. Then $\text{Pr}_{27}(\cdot)$ is computed as

$$\text{Pr}_{27}(\cdot) \triangleq \text{Pr}_{25}\left(S^t|U_w^{(t)}, U_n^{(t)}, S^{(t-1)}, U_w^{(t-1)}, U_n^{(t-1)}\right) \text{Pr}_{16}\left(U_w^{(t)}, U_n^{(t)}|U_w^{(t-1)}, U_n^{(t-1)}\right). \quad (35)$$

To compute $\text{Pr}_{12}(\cdot)$ in (33) and $\text{Pr}_{15}(\cdot)$ in (34), we need to derive $\text{Pr}_{25}(\cdot)$. For the derivation of $\text{Pr}_{25}(\cdot)$, to avoid prohibitive complexity of calculation, we consider two specific cases. The first case is that there is no change for the number of WPU and NPU between time $t - 1$ and t . This case is expected to happen most frequently because the PU generally has longer inter-arrival time and packet length than the frame size of the SUs. The second case is that the numbers of WPU and NPU are reduced as time goes from $t - 1$ to t . If the PU activity is not too high, this case happens when some of the existing PUs disappear and no new PU enters into the subchannels. Then subchannels detected as idle at time $t - 1$ still remains idle even at time t , which can affect the sensing stage significantly. For the other cases, we use a general approach. Depending on the changes of the numbers of the PUs, $\text{Pr}_{25}(\cdot)$ is derived as

$$\text{Pr}_{25}(\cdot) \cong \begin{cases} \text{Pr}_{25a}(H), & U_w^{(t)} = U_w^{(t-1)}, U_n^{(t)} = U_n^{(t-1)}, \\ \text{Pr}_{25b}(H), & U_w^{(t)} \leq U_w^{(t-1)}, U_n^{(t)} \leq U_n^{(t-1)}, \\ \text{Pr}_{25c}(H), & \text{otherwise}, \end{cases} \quad (36)$$

where $H = \{S^{(t)}|U_w^{(t)}, U_n^{(t)}, S^{(t-1)}, U_w^{(t-1)}, U_n^{(t-1)}\}$. To analyze the first case in (36), where there is no change in the number of WPU and NPU between time $t - 1$ and t , we reuse the assumption that there is no change in the positions at subchannels of the NPUs for the same number of NPUs at times t and $t - 1$, see Section III-B. With this approximation, under the condition that there exists at least one channel at time $t - 1$, i.e. $S^{(t-1)} < 2$, there should also exist at least one idle channel at time t , i.e. $S^{(t)} < 2$. Thus, if no false alarm occurs, only coarse sensing is performed, i.e. $S^{(t)} = 0$ and otherwise $S^{(t)} = 1$. Next, for the condition that no channel is detected as idle at time $t - 1$, i.e. $S^{(t-1)} = 2$, there can be a large number of possible events depending on the positions of NPUs and false alarms. Thus, instead of considering all the possible events, we consider two cases and apply approximations for each one. The first case is that there exists a small number of NPUs at time $t - 1$ so that the NPUs can not occupy all $X - U_w^{(t-1)}$ channels, i.e. $f_s\left(U_n^{(t-1)}, X - U_w^{(t-1)}, \lfloor Y/l_n \rfloor\right) = 0$. In this case, because there exists at least one idle channel, we approximate that the SU performs fine sensing and detects the idle channel at time t , i.e. $S^{(t)} = 1$. In contrast, for the second case where there exists enough NPUs such that they are spread over all $X - U_w^{(t-1)}$ channels, i.e. $f_s\left(U_n^{(t-1)}, X - U_w^{(t-1)}, \lfloor Y/l_n \rfloor\right) > 0$, we approximate that all channels are detected as busy at time t , i.e. $S^{(t)} = 2$. Considering all these sub-cases, we derive $\text{Pr}_{25a}(\cdot)$

as

$$\Pr_{25a}(\cdot) \triangleq \begin{cases} (1 - \phi_a)^Y, & S^{(t)} = 0, S^{(t-1)} < 2; \\ 1 - (1 - \phi_a)^Y, & S^{(t)} = 1, S^{(t-1)} < 2; \\ 1, & S^{(t)} = 2, J^{(t-1)} > 0, \text{ or } S^{(t)} = 1, J^{(t-1)} = 0; \\ 0, & \text{otherwise,} \end{cases} \quad (37)$$

where $J^{(x)} = f_s(U_n^{(x)}, X - U_w^{(x)}, \lfloor Y/l_n \rfloor)$. Next, we analyze the second case in (36), i.e. $U_w^{(t)} \leq U_w^{(t-1)}$ and $U_n^{(t)} \leq U_n^{(t-1)}$, which implies that the number of PUs decreases. Similar to the first case in (36), if there exist idle channels at time $t - 1$, i.e. $S^{(t-1)} < 2$, there must also exist idle channels at time t , i.e. $S^{(t)} < 2$. If a false alarm does not occur on any of the Y subchannels in a channel utilized for data transmission, the SU performs only coarse sensing, i.e. $S^{(t)} = 0$, and otherwise, $S^{(t)} = 1$. On the other hand, for the condition that there is no idle channel at time $t - 1$, i.e. $S^{(t-1)} = 2$, the probability of the sensing stage at time t is calculated by dividing the number of the cases that $U_n^{(t)}$ NPU's occupy exactly all $X - U_w^{(t)}$ channels, $f_s(U_n^{(t)}, X - U_w^{(t)}, \lfloor Y/l_n \rfloor)$, by the number of all possible cases $\binom{(X - U_w^{(t)}) \lfloor Y/l_n \rfloor}{U_n^{(t)}}$. Note that when $S^{(t-1)} = 2$, it is not possible to perform only the coarse sensing at time t , because the channel that is going to be utilized for data transmission is not determined. In other words, the probability of $S^{(t-1)} = 0$ under $S^{(t-1)} = 2$ equals zero. As a result, the probability of $S^{(t-1)} = 1$ under $S^{(t-1)} = 2$ equals to one minus the probability of $S^{(t-1)} = 2$ under $S^{(t-1)} = 2$. Thus, we derive $\Pr_{25b}(\cdot)$ as

$$\Pr_{25b}(\cdot) \triangleq \begin{cases} (1 - \phi_a)^Y, & S^{(t)} = 0, S^{(t-1)} < 2; \\ 1 - (1 - \phi_a)^Y, & S^{(t)} = 1, S^{(t-1)} < 2; \\ \frac{J^{(t)}}{\binom{(X - U_w^{(t)}) \lfloor Y/l_n \rfloor}{U_n^{(t)}}}, & S^{(t)} = 2, S^{(t-1)} = 2; \\ 1 - \frac{J^{(t)}}{\binom{(X - U_w^{(t)}) \lfloor Y/l_n \rfloor}{U_n^{(t)}}}, & S^{(t)} = 1, S^{(t-1)} = 2, \\ 0, & \text{otherwise.} \end{cases} \quad (38)$$

Finally, we compute $\Pr_{25c}(\cdot)$ in (36). In this case, again to simplify the computation, we ignore the effect of the sensing stage at time $t - 1$ and only focus on the sensing stage at time t . Then, we compute the probability that the SU performs only coarse sensing, i.e. $S^{(t)} = 0$, by dividing the number of cases that at least one channel remains idle and no false alarm occurs on that channel, $(1 - \phi_a)^Y \binom{(X - U_w^{(t)} - 1) \lfloor Y/l_n \rfloor}{U_n^{(t)}}$, by all possible cases of all channels remaining idle, $\binom{(X - U_w^{(t)}) \lfloor Y/l_n \rfloor}{U_n^{(t)}}$. On the other hand, the probability that the SU detects no idle channel, i.e. $S^{(t)} = 2$, is calculated by considering the case that U_n NPU's occupy exactly all $X - U_w^{(t)}$ channels, i.e. $f_s(U_n^{(t)}, X - U_w^{(t)}, \lfloor Y/l_n \rfloor)$. Note that for the case that there

appears too many NPUs on the spectrum so that there is no possibility that even one channel cannot remain idle, only $S = 2$ is feasible. This case can be denoted as $V = (X - U_w^{(t)} - 1)\lfloor Y/l_n \rfloor$, because $X - U_w^{(t)}$ channels are available for the NPU and each channel can have a maximum $\lfloor Y/l_n \rfloor$ NPUs.

Considering all these cases, we have

$$\Pr_{25c}(\cdot) \triangleq \begin{cases} \frac{(1-\phi_a)^Y \binom{(X-U_w^{(t)}-1)\lfloor Y/l_n \rfloor}{U_n^{(t)}}}{\binom{(X-U_w^{(t)})\lfloor Y/l_n \rfloor}{U_n^{(t)}}}, & S^{(t)} = 0, U_n^{(t)} \leq V; \\ \frac{J^{(t)}}{\binom{(X-U_w^{(t)})\lfloor Y/l_n \rfloor}{U_n^{(t)}}}, & S^{(t)} = 2, U_n^{(t)} \leq V; \\ 1 - \Pr_{25c}(S^{(t)} = 0|\cdot) - \Pr_{25c}(S^{(t)} = 2|\cdot), & S^{(t)} = 1, U_n^{(t)} \leq V; \\ 1, & S^{(t)} = 2, U_n^{(t)} > V; \\ 0, & \text{otherwise.} \end{cases} \quad (39)$$

IV. NUMERICAL RESULTS

In this section we provide performance results for all the considered protocols. We note that all analytical results were verified via simulations using a method of batch means for 90% confidence interval. Each simulation run, with a warm-up period of 10000 network events, was divided into 100 batches, where each batch contained 10000 network events.

Before we proceed with the presentation we need to comment on the calculation of C . Following the IEEE P802.22 model [12] we consider the PHY capacity C_p and MAC layer overhead ξ separately, such that $C = (1 - \xi)C_p$. For the PHY subchannel capacity C_p , we assume that 16-QAM modulation is used, which can transmit 4 bits per OFDM symbol, with 1/2 channel coding per subcarrier. Then the number of transmitted bits per OFDM symbol per subcarrier is $4 \times 1/2 = 2$. Note that for the IEEE P802.22 system one channel consists of 60 subchannels each of which is again composed of 24 subcarriers, except for pilot carriers. In order to reduce the complexity of calculation, as well as provide a reasonable guard band for NPUs, we assume that six subchannels of IEEE P802.22 represents one subchannel in the system model for our analysis. In other words, in our analysis one channel consists of 10 subchannels, each of which is composed of $24 \times 6 = 144$ subcarriers. Also, we assume that uplink and downlink is time division duplexed, where 16 symbols and 8 symbols are assigned to downlink and uplink, respectively. Focusing on the downlink throughput, we calculate the PHY capacity as $C_p = 16 \text{ (symbols)/10 ms (frame length)} \times 2 \text{ (bits/symbol/subcarrier)} \times 144 \text{ (subcarriers/subchannel)} = 460.8 \text{ kbps}$.

For the MAC layer overhead ξ we consider the frame structure of the IEEE P802.22 such that one downlink OFDM symbol of all subchannels is assigned to a preamble and two downlink OFDMA symbols

of all subchannels are assigned to management messages. Also considering errors on the subchannels, we assume a bit error rate of 10^{-6} . Hence, we calculate the MAC layer overhead reduction factor as $1 - \xi = 13/16 \times (1 - 10^{-6}) = 0.8125$. Therefore the total subchannel capacity is $C = (1 - \xi)C_p = 460.8 \text{ kbps} \times 0.8125 = 374.4 \text{ kbps}$.

Due to many parameters considered we limit our numerical investigation to three most representative case studies. That is, we consider the impact of varying number of NPUs, the impact of varying PU activity and the impact on two-stage spectrum sensing design on the system throughput. Results are presented in Section IV-A, Section IV-B and Section IV-C, respectively.

A. Impact of Varying Number of NPUs on OS-OFDMA Design

Throughout this section we assume that $X = 4$ channels are available and split into $Y = 10$ subchannels. Frame length is set to $t_f = 20 \text{ ms}$, which represents the length of two frames of IEEE P802.22 [12]. False alarm and detection probability for the coarse sensing case is $\delta_a = 0.99$ and $\phi_a = 0.1$, respectively, while for the fine sensing case $\delta_a = 1$ and $\phi_a = 0$, respectively. Sensing time during coarse sensing is $\tau_a = 0$. Since we have assumed that uplink and downlink are divided by time division duplex and coarse sensing is performed in the uplink, as in [12], the sensing overhead is zero. In the fine sensing phase $\tau_f = \frac{3}{5}t_f$, modeling 3 consecutive frames used for the fine sensing and the following 2 frames used for data transmission until next sensing period. In this section we do not couple values of δ_a , δ_f , ϕ_a and ϕ_f with the spectrum sensing PHY parameters, like the SNR or the sensing threshold. Instead, we assume that a certain values of detection and false alarm probabilities are realizable. More detailed investigation of spectrum sensing layer considering relation between sensing PHY and the rest of the protocol stack, as seen in Fig. 1, will be presented in Section IV-C. Furthermore we assume that $l_c = 1$, $l_w = 10$, $l_n = 1$ subchannels are allocated to CBR, NPU and WPU connection, respectively. Note that the number of subchannels assigned to VBR connection, l_v , is varying depending on the network state. The maximum number of users of each class is $U_{v,\max} = 2$, $U_{c,\max} = 10$ and $U_{w,\max} = 2$ (investigating impact of NPUs), and $U_{v,\max} = 2$, $U_{c,\max} = 10$ and $U_{n,\max} = 10$ (investigating impact of WPUs).

Also, for the purpose of this section we set up inter-arrival and departure times taking into consideration IEEE P802.22 network, where many active licensed incumbents operate over the TV band. Since in general, the traffic pattern of PUs for such case is not well known (more discussion on this aspect is presented in Section IV-B), for the WPU we keep the wireless assist video devices [25] in mind, which can be assumed to broadcast on average four hours of signal transmission for every twelve hours on average in this scenario. For the NPU, we consider environment with numerous wireless microphones and assume

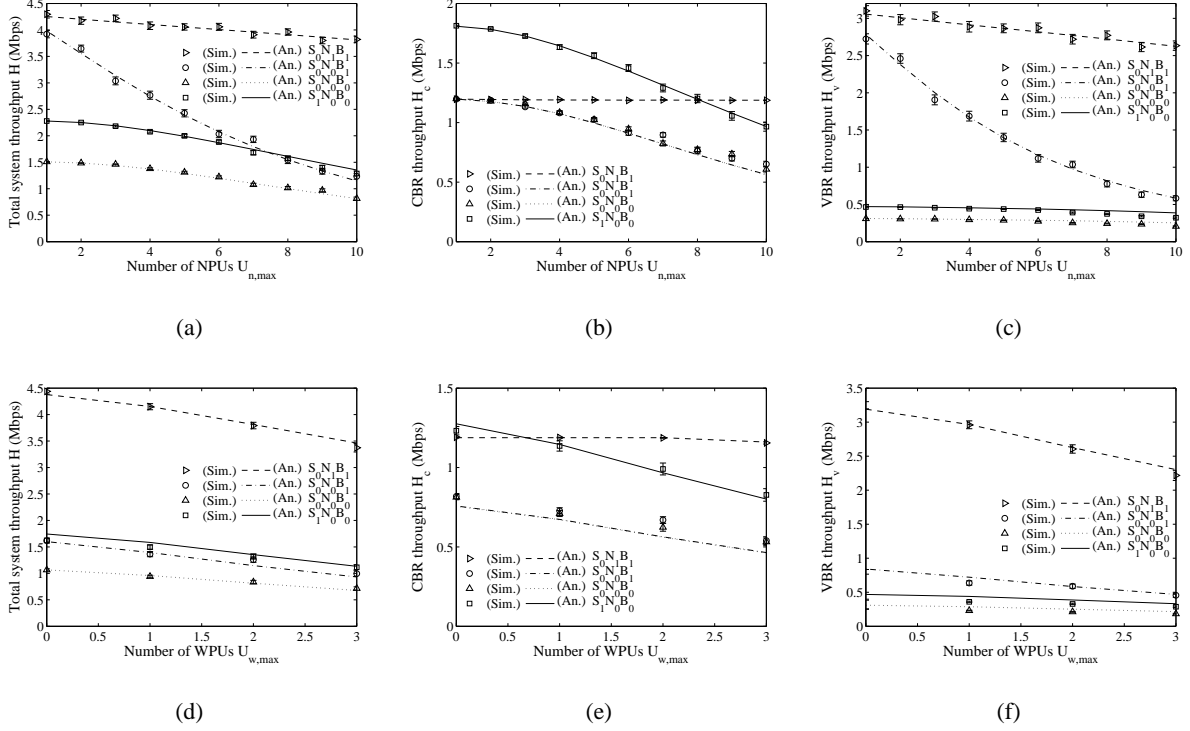


Fig. 2. Performance of different OS-OFDMA options as a function of NPU, Fig. (a), (b), (c), and WPU, Fig. (d), (e), (f) for $X = 4$, $Y = 10$, $M = 40$, $t_f = 20$ ms, $\delta_a = 0.99$, $\phi_a = 0.1$, $\tau_a = 0$, $\delta_f = 1$, $\phi_f = 0$, $\tau_f = \frac{3}{5}t_f$, $C = 374.4$ kbps, $U_{w,\max} = 2$ (WPU), $U_{n,\max} = 10$ (NPU), $l_w = 10$, $l_n = 1$, $U_{c,\max} = 10$, $l_c = 1$, $U_{v,\max} = 2$; (a) (d) total system throughput, (b) (e) throughput of CBR connections, and (c) (f) throughput of VBR connections.

that they appear every two hours on average and utilize channels for one hour on average. For CBR, considering voice or video transmission, we assume that on average five minute long CBR connection is generated for every five minutes on average. For VBR, we assume that data traffic is generated every two hours on average and continues for two hours if one channel is assigned for a VBR connection. For simulation efficiency, since we operate in large parameter ranges, we scale them down by setting the CBR connection arrival rate to one second with preserving the ratios between all traffic parameters, i.e. we normalize average inter-arrival and departure times of all users in the unit of five minutes by dividing them by 300 seconds. Thus for the large number of users, the inter-arrival time becomes shorter. For the analysis, we calculate the inter-arrival time by dividing the individual inter-arrival time by the maximum number of users. In summary, $1/\lambda_w = 144/U_{w,\max}$ s, $1/\lambda_n = 24/U_{n,\max}$ s, $1/\lambda_c = 1/U_{c,\max}$ s, $1/\lambda_v = 12/U_{v,\max}$ s, $1/\mu_w = 48$ s, $1/\mu_n = 12$ s, $1/\mu_c = 1$ s and $1/\mu_v = 240$ s.

The results are presented in Fig. 2. Obviously the throughput of every OS-OFDMA design option

decreases with increasing numbers of NPUs and WPU. First, we observe that $S_0N_1B_1$ is the best design option when total and VBR throughput is concerned, which is due to the highest flexibility in exploring all spectrum opportunities. Second, interestingly with low number of NPU and WPU CBR throughput is higher for $S_1N_0B_0$ than for $S_0N_1B_1$, while with the high number of WPU and NPU the opposite holds, see Fig. 2(b) and Fig. 2(e). This is because of the sensing overhead of the fine sensing that is performed more frequently for $S_0N_1B_1$ than for $S_1N_0B_0$. Third, there is no difference in CBR throughput between $S_0N_0B_1$ and $S_0N_0B_0$ when the number of NPUs varies. This is because in this network setup CBR, which has higher priority than the VBR, utilizes enough resources even though channel bonding is not applied. Fourth, the $S_0N_0B_1$ design option is extremely sensitive to the activity of the NPUs. The throughput of this design option decreases rapidly as the number of NPUs increases, compare Fig. 2(a) with Fig. 2(c). This effect is not visible however when the NPU number is kept fixed, but the number of WPUs changes, see Fig. 2(d) and Fig. 2(f) and compare with Fig. 2(a) and Fig. 2(c), respectively. This is because $S_0N_0B_1$ is sensitive to the position of NPUs in the spectrum.

An interesting observation is that the total throughput of $S_1N_0B_0$ is greater than that of $S_0N_0B_1$ for large number of NPUs and WPUs, see Fig. 2(a) and Fig. 2(d), even though the implementation for $S_0N_0B_1$ enables wider bandwidth sensing than $S_1N_0B_0$. This is because for $S_0N_0B_1$, due to channel bonding, the probability that OSA network needs to sense the channel is much higher and network needs to perform sensing often. While for $S_1N_0B_0$ only actively used channel is sensed.

Note that the simulation results agree with the analysis in all figures. A slight mismatch between simulation and analysis for cases $S_0N_0B_1$, $S_0N_0B_0$ and $S_1N_0B_0$ in Fig. 2(e) is a result of the approximation used in calculating throughput for these design options. More discussion on this issue is presented in Section IV-B.

B. Impact of PU Activity on OS-OFDMA Design

To investigate the impact of varying PU activity on the performance of different OS-OFDMA designs, for ease of explanation, we have considered to focus on NPUs only. Then, as a case study, we consider wireless microphones as an example of NPU. The parameters of the OS-OFDMA are the same as in Section IV-A. Before presenting the performance results we need to estimate the most realistic values of wireless microphones activity descriptors, i.e. average arrival rate and channel occupancy time.

In the case of average NPU channel occupancy time we set it to a value between one and four hours, believing this represents a common activity time. More discussion is needed, however, on the arrival rate of the wireless microphones. Since the potential number of wireless microphones is location dependent,

TABLE III
SCENARIOS FOR THE ANALYSIS OF NPU ACTIVITY IMPACT ON THE PERFORMANCE OF OS-OFDMA DESIGNS

Nickname	“heavy urban”	“urban”	“light urban”	“event”
Location in US	Los Angeles, CA	Santa Barbara, CA	Madison, WI	Staples Center, CA
Users/mi ² , ρ	7452.7	4708.2	2701.0	7452.7
Users/one NPU, $1/h$	3000	3000	3000	3000
Cell diameter, L mi	2	2	2	2
Velocity, v mph	1.5	1.5	1.5	1.5
Dwell time, $1/\mu_n$ h	1	1	1	4
$U_{n,\max}$	8	5	3	18

we have setup four different network scenarios, representing different places in the USA, see Table III, that differ in, e.g., population density ρ . We assume that OS-OFDMA BS covers a fraction of the area of diameter L of the considered location, while the wireless microphones move in and out of the BS circular coverage with a certain speed v . Then using a fluid flow model approximation [26] we compute the average crossing rate of the wireless microphones to that area and translate it directly to an average arrival rate of wireless microphone on any of the subchannels. That is $\lambda_n = \rho h \pi L v$, where $1/h$ denotes number of inhabitants per one active wireless microphone in the considered location. Since the value of h is not known reliably⁵ we assume that one wireless microphone is present per 300 inhabitants and such wireless microphone is active for 10% of the time. Finally, $U_{n,\max} = \max(\lfloor \pi (L/2)^2 \rho h \rfloor, 1)$ in this case. We set the inter-arrival and departure times for other users as the same value as Section IV-A. Also for analysis, we normalize all time parameters in the unit of five minutes as in Section IV-A.

The results are grouped separately for total average network throughput, CBR throughput and VBR throughput, see Fig. 3, Fig. 4 and Fig. 5, respectively. We have chosen to vary number of CBR connections in all figures as a parameter, since in our model CBR connection is the most quality of service sensitive and capacity demanding SU traffic class. First we immediately observe that $S_0N_1B_1$ implementation obtains the highest throughput. The larger the activity of the wireless microphones, the bigger the difference between $S_0N_1B_1$ and the remaining implementations – compare for example Fig. 3(c) and Fig. 3(d). Option $S_0N_1B_1$ obtains a throughput around 3 Mbps, even in the “event” scenario. This is due to maximum

⁵The only credible report we were able to find was [27]. The estimation using data present in this report was based on a simple calculation. According to [27, Sec. A2] there were 1924431 wireless microphone shipments in the European Union (EU) between 2002 and 2006, which translates to ≈ 1 wireless microphone per 1000 EU inhabitants (assuming a constant level of wireless microphone shipments per year).

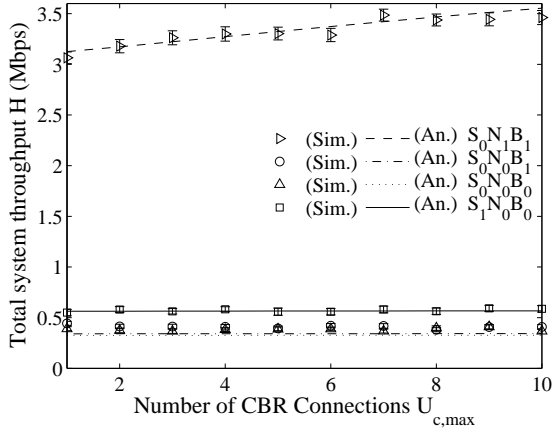
utilization of the remaining channel capacity by subchannel notching and channel bonding. As the NPU activity increases all implementations reach almost zero throughput, while $S_0N_1B_1$ still obtains reasonable performance. The worst performance is obtained for $S_0N_0B_0$, while the $S_1N_0B_0$ and $S_0N_0B_1$ are somehow in between the extreme cases. As the activity of the wireless microphones decreases all implementations start to converge in throughput – compare for example Fig. 4(a) with Fig. 4(c), however the individual relation between the implementations stays the same. Then, we observe that all implementations except $S_0N_1B_1$ obtain a similar throughput, irrespective of the network scenario. This proves that subcarrier notching promises to deliver most of the available capacity in the licensed bands. Note that total and CBR throughput increases as the number of CBR connections increase, while VBR throughput obviously goes down, since most of the capacity is taken by the CBR connections.

The worst situation, in terms of network scenario, is the “event” scenario. Due to long channel dwell time by NPU, i.e. four hours, the throughput for all implementations except $S_0N_1B_1$ reaches zero. We also conclude that in scenarios where the activity of the wireless microphones is low, like in the “light urban” scenario, the users of systems based on OS-OFDMA are promised to obtain high quality of service, see Fig. 3(c), Fig. 4(c) and Fig. 5(c), irrespective of the implementation.

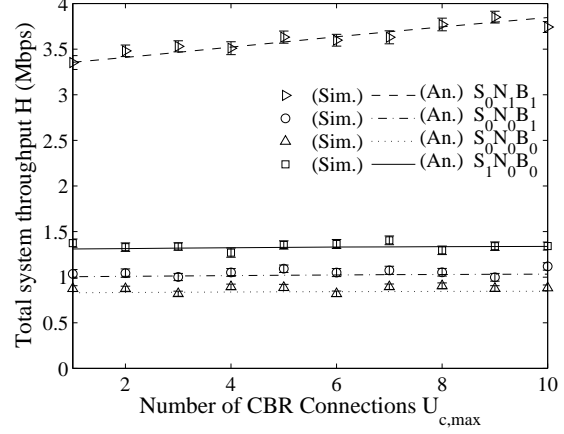
A separate comment is needed for simulation verification of the results. In all cases $S_0N_1B_1$ implementation matches simulations perfectly, irrespective of the parameters selected. However, due to the approximations assumed for the remaining OS-OFDMA implementations the slight discrepancy is particularly visible for the scenarios with high NPU activity rate, compare for example Fig. 4(a) with Fig. 4(c). The results prove, on the other hand, that the developed model works very well for low PU activities, which is the typical case in real life PU occupancy statistics [2], [17]. Still, for each case study the relation between each OS-OFDMA implementation is well captured for any value of the parameters considered, while for the majority of the cases the mismatch between simulations and analysis is less than 10%.

C. Impact of Two-stage Spectrum Sensing Options on OS-OFDMA Design

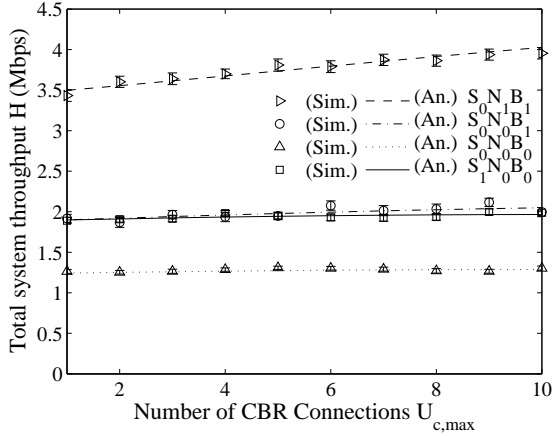
The final experiment considers effect of sensing design parameters on the performance of OS-OFDMA designs. For this investigation we change the sensing time of coarse sensing, which has a direct effect on false alarm probability and makes a significant impact on the frequency of switching to fine sensing (and as a result on the throughput of the system). We keep other parameters the same as in the first experiment described in Section IV-A, except $U_{n,\max} = 2$, to see the effect of coarse sensing clearer, and $U_{c,\max} = 10$. We do not alter parameters of fine sensing phase, since we want to explore the benefit of



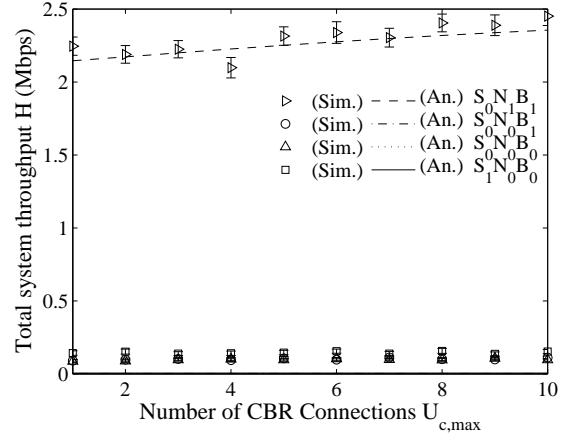
(a) “heavy urban”



(b) “urban”



(c) “light urban”



(d) “event”

Fig. 3. Total throughput of different OS-OFDMA implementations for all network cases; Parameter setup and the ordering of the figures is the same as in Fig. 2: (a) “heavy urban”, (b) “urban”, (c) “light urban”, (d) “event”.

two-stage sensing and the coarse sensing phase is a common element of every sensing method, including single stage sensing.

Considering Rayleigh Channel with Additive White Gaussian Noise, we compute false alarm probability, p_{10} , and detection probability, p_{11} , for an individual SU user as [16, Eq. (3)] and [16, Eq. (4)], respectively. Then, according to [16, Sec. III-B], we can derive p_{11} as a function of p_{10} and τ_a for given average PU SNR and subchannel bandwidth b . Assuming collaborative sensing of all CBR and VBR users and OR logic for combining scheme, we compute system false alarm probability as

$$\phi_a = 1 - (1 - p_{10})^{(U_{c,\max} + U_{v,\max})}, \quad (40)$$

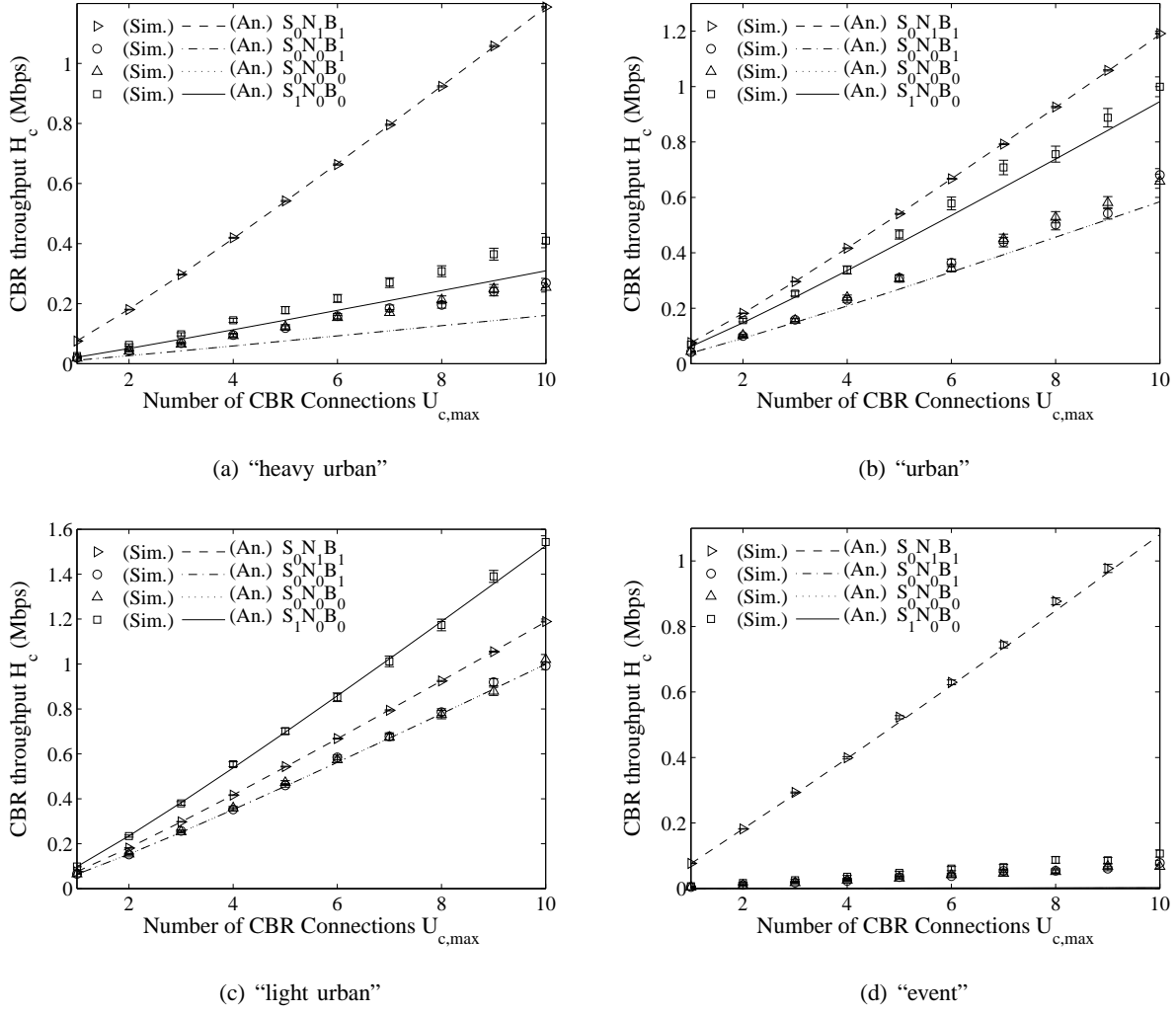
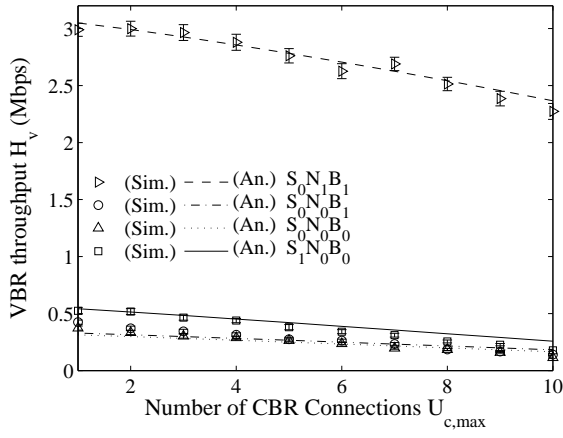


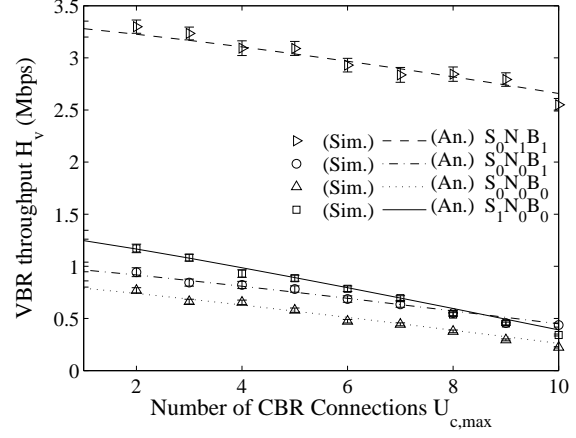
Fig. 4. CBR throughput of different OS-OFDMA implementations for all network cases. Parameter setup and the ordering of the figures is the same as in Fig. 2.

and system detection probability, δ_a , as (40) replacing p_{10} with p_{11} . In this evaluation we keep the detection probability $\delta_a = 0.99$ and change the sensing time for the coarse sensing such that $\tau_a = (0, 4)$ ms. Note that zero sensing time represents single stage sensing. Table IV presents calculated false alarm probability, ϕ_a , based on the assumed sensing time τ_a .

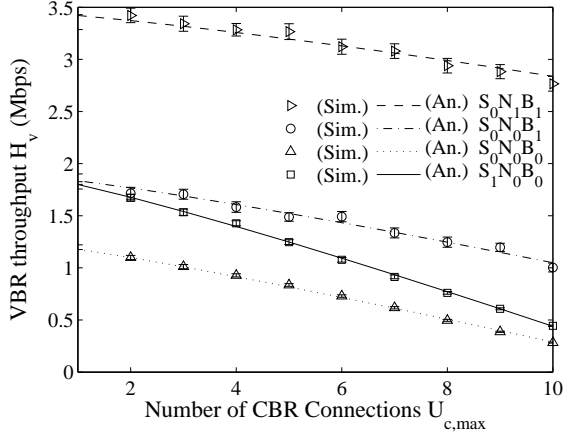
The results are presented in Fig. 6. First interesting observation is that two stage sensing does not always show better performance than single stage sensing. Comparing the total throughput at $\tau_a = 0$ with $\tau_a \approx (0.5, 1)$ ms of all OS-OFDMA options, two stage sensing shows worse performance than single stage sensing. This result is due to high probability of false alarm for this range of τ_a , see Table IV. In



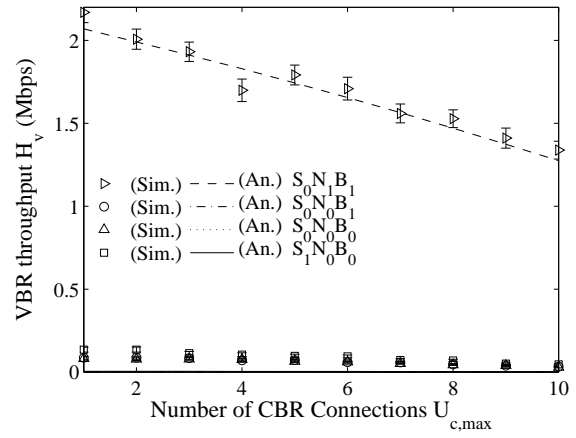
(a) “heavy urban”



(b) “urban”



(c) “light urban”



(d) “event”

Fig. 5. VBR throughput of different OS-OFDMA implementations for all network cases. Parameter setup and the ordering of the figures is the same as in Fig. 2.

TABLE IV

SENSING TIME AND THE RESPECTIVE FALSE ALARM PROBABILITY FOR THE EXPERIMENT INTRODUCED IN SECTION IV-C

τ_a (ms)	0	0.5	1	1.5	2	2.5	3	3.5	4
ϕ_a	1	0.2308	0.0446	0.0087	0.0018	0.0004	0.0001	1.57e-4	0.333e-4

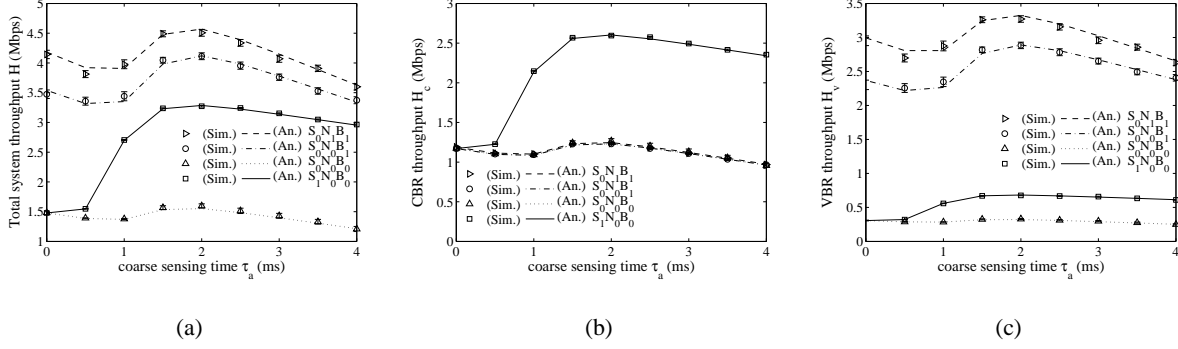


Fig. 6. Throughput of OS-OFDMA implementations, (a) total, (b) CBR, and (c) VBR, as a function of coarse sensing time. Parameter setup is the same as in Fig. 2, except for $U_{n,\max} = 2$, $U_{c,\max} = 10$ while τ_a and ϕ_a are given in Table IV.

addition, for this network setup, the throughput is maximized at $\tau_a = 2$ ms and is larger than for $\tau_a = 0$ which confirms that two-stage sensing can indeed benefit all OS-OFDMA operations. This also confirms that the design choice of IEEE P802.22 for spectrum sensing method was correct. When τ_a increases beyond the point for which the throughput is largest, the throughput of all OS-OFDMA implementations starts to rapidly decrease. This is due to the fact that the sensing overhead starts to dominate over potential improvement from decreased false alarm rate. This so called sensing-throughput tradeoff is in agreement with a similar investigation in the context of OSA ad hoc networks [16]. Note that the relation between sensing time and the obtained throughput are the same when looking at total, CBR and VBR throughput, see the shapes of all curves in Fig. 6(a), Fig. 6(b) and Fig. 6(c). Also, the different order in obtained throughput for each OS-OFDMA implementation are due to the specific OS-OFDMA options, not due to spectrum sensing parameters selected. For that, compare, e.g., the position of $S_1N_0B_0$ in Fig. 6(a) with the position of the same implementation in Fig. 6(b). For more on this aspect please refer to Section IV-B. Finally, note that the simulation results match well with the analysis for all OS-OFDMA implementations.

V. CONCLUSIONS

In this paper we have proposed an analytical model that allows the comparison of different designs of OS-OFDMA. We have considered design options that include channel bonding, subchannel notching and two stage spectrum sensing. As a performance metric we have derived average throughput obtained by the secondary users of the spectrum. In the analysis we have included the inter-relations of different connection classes and priorities, like constant and variable bit rate traffic of the secondary users, and wideband and narrowband primary users. We concluded that OS-OFDMA design that allows the flexible bonding of channels and notching of subchannels currently occupied by the primary users, obtains the

highest throughput in comparison to the designs that do not consider those options. As one of our numerical results show, the improvement reaches couple of hundred percent when the activity level of the different primary user types is very high. Also, as our investigation show, the two-stage spectrum sensing technique used in OS-OFDMA proves to increase the average network throughput, provided the probability of false alarm in the coarse sensing stage is low.

APPENDIX A

DERIVATION OF $G_x(k|U_x)$ AND $T_x(j|\mu_x)$

If the inter-arrival time has a negative exponential distribution with average arrival rate λ_x , the number of connections generated in a frame of length t_f has a Poisson distribution. However, because we limit the maximum number of users to $U_{x,\max}$, the number of users including newly generated connections, U_x , cannot exceed $U_{x,\max}$. Considering this, we derive the probability of k new connections being generated in a frame, $G_x(k|U_x)$, as

$$G_x(k|U_x) \triangleq \begin{cases} \frac{(\lambda_x t_f)^k e^{-\lambda_x t_f}}{k!}, & k \geq 0, U_x < U_{x,\max}; \\ \sum_{i=k}^{\infty} \frac{(\lambda_x t_f)^i e^{-\lambda_x t_f}}{i!}, & k \geq 0, U_x = U_{x,\max}; \\ 0, & k < 0. \end{cases} \quad (41)$$

Note that the subscript $x = \{w, n, c, v\}$ indicates the class of users, i.e., w for WPU, n for NPU, c for CBR, and v for VBR.

Further, denoting the departure rate of each connection as μ_x , the probability that j connections are released from U_x active connections during a frame of length t_f , $T_x(j|m_x, \mu_x, t_f)$, can be calculated recursively as

$$T_x(j|U_x, \mu_x, t_f) \triangleq \begin{cases} \int_0^{t_f} m_x \mu_x e^{-U_x \mu_x t} T_x(j-1|U_x-1, \mu_x, t_f-t) dt, & j > 0; \\ e^{-U_x \mu_x t_f}, & j = 0, \end{cases} \quad (42)$$

which after some manipulation reduces to

$$T_x(j|U_x, \mu_x, t_f) = \binom{U_x}{j} e^{-U_x \mu_x t_f} (e^{\mu_x t_f} - 1)^j. \quad (43)$$

Since we only consider the connection release probability for $U_x = U_x^{(t-1)}$ users within the duration of a frame we abbreviate $T_x(j|\mu_x) \triangleq T_x(j|U_x^{(t-1)}, \mu_x, t_f)$.

APPENDIX B

DERIVATION OF $f_s(k, x, r)$

First we introduce the supporting variable, i_j – the number of items in j -th bin where $j \in \{1, \dots, x\}$. Then, there can be $\binom{r}{i_j}$ possible distributions for the j -th bin, and thus for x bins there can be $\sum_{j=1}^{i_1} \binom{r}{j} \cdots \sum_{j=1}^{i_x} \binom{r}{j}$ possibilities. Because there should be no bin empty, $i_j \geq 1$. Also, each of the bins has a capacity of r items and the total number of items cannot be greater than k , and therefore $i_j \leq \min(r, k)$. In addition, if the number of bins is less than the number of items or equal to zero, there is no way to fill all x bins. Thus

$$f_s(k, x, r) = \begin{cases} \sum_{\mathcal{I}(k, x, r)} \sum_{j=1}^{i_1} \binom{r}{j} \cdots \sum_{j=1}^{i_x} \binom{r}{j}, & 0 < x < k; \\ 0, & \text{otherwise,} \end{cases} \quad (44)$$

where $\mathcal{I}(k, x, r) = \{i_1, \dots, i_x \mid \sum_{j=1}^x i_j = k, i_1, \dots, i_x \in \{1, \dots, \min(r, k)\}\}$.

ACKNOWLEDGEMENT

We would like to thank former and current members of the IEEE P802.22 committee for important suggestions and discussions, in particular Winston Caldwell, Gerald Chouinard, Carlos Cordeiro, Wendong Hu, Saishankar Nandagopalan, Steve Shellhammer, Carl R. Stevenson, Jianfeng Wang and Lei Zhongding. We would also like to thank Jasper Goseling and Jos Weber from TU Delft for helpful discussions.

REFERENCES

- [1] J. Park, P. Pawełczak, P. Grønsund, and D. Čabrić, “Performance of opportunistic spectrum OFDMA network with users of different priorities and traffic characteristics,” in *Proc. IEEE GLOBECOM*, Miami, FL, USA, Dec. 6–10, 2010.
- [2] G. Staple and K. Werbach, “The end of spectrum scarcity,” *IEEE Spectr.*, vol. 41, no. 3, pp. 48–52, Mar. 2004.
- [3] Q. Zhao and B. M. Sadler, “A survey of dynamic spectrum access: Signal processing, networking, and regulatory policy,” *IEEE Signal Processing Mag.*, vol. 24, no. 3, pp. 79–89, May 2007.
- [4] P. Pawełczak, S. Pollin, H.-S. W. So, A. Bahai, R. V. Prasad, and R. Hekmat, “Quality of service of opportunistic spectrum access: A medium access control approach,” *IEEE Wireless Commun. Mag.*, vol. 15, no. 5, pp. 20–29, Oct. 2008.
- [5] L. Nuyami, *WiMAX: Technology for Broadband Wireless Access*. Hoboken, NJ, USA: Wiley, 2007.
- [6] *Draft Standard for Local and Metropolitan Area Networks: Standard Air Interface for Mobile Broadband Wireless Access Systems Supporting Vehicular Mobility: Physical and Media Access Control Layer Specification*, IEEE Std. P802.20 Draft 3.0, Mar. 2007.
- [7] D. Astély, E. Dahlman, A. Furuskär, Y. Jading, M. Lindström, and S. Parkvall, “LTE: The evolution of mobile broadband,” *IEEE Commun. Mag.*, vol. 47, no. 4, pp. 44–51, Apr. 2009.
- [8] T. A. Weiss and F. K. Jondral, “Spectrum pooling: an innovative strategy for the enhancement of spectrum efficiency,” *IEEE Commun. Mag.*, vol. 42, no. 3, pp. S8–S14, Mar. 2004.

- [9] D. T. Ngo, C. Tellambura, and H. H. Nguyen, "Resource allocation for OFDMA-based cognitive radio multicast networks with primary user activity consideration," *IEEE Trans. Veh. Technol.*, vol. 59, no. 4, pp. 1668–1679, May 2010.
- [10] A. E. Leu, B. L. Mark, and M. A. McHenry, "A framework for cognitive WiMAX frequency agility," *Proc. IEEE*, vol. 97, no. 4, pp. 755–773, Apr. 2009.
- [11] Y. Zhang and C. Leung, "Resource allocation for non-real-time services in OFDM-based cognitive radio systems," *IEEE Commun. Lett.*, vol. 13, no. 1, pp. 16–18, Jan. 2009.
- [12] *Draft Standard for Wireless Regional Area Networks Part 22: Cognitive Wireless RAN Medium Access Control (MAC) and Physical Layer (PHY) Specifications: Policies and Procedures for Operation in the TV Bands*, IEEE Std. P802.22 Draft 3.0, Apr. 2010.
- [13] C. R. Stevenson, G. Chouinard, Z. Lei, W. Hu, S. J. Shellhammer, and W. Caldwell, "IEEE 802.22: The first cognitive radio wireless regional area network standard," *IEEE Commun. Mag.*, vol. 47, no. 1, pp. 130–138, Jan. 2009.
- [14] L. Song, C. Feng, Z. Zeng, and X. Zhang, "Research on WRAN system level simulation platform design," in *Proc. ICST Chinacom*, Hangzhou, China, Aug. 25–27, 2008.
- [15] S.-E. Elayoubi and B. Foursité, "Performance evaluation of admission control and adaptive modulation in OFDMA WiMax systems," *IEEE/ACM Trans. Networking*, vol. 16, no. 5, pp. 1200–1211, Oct. 2008.
- [16] J. Park, P. Pawełczak, and D. Čabrić. (2009) Performance of joint spectrum sensing and MAC algorithms for multichannel opportunistic spectrum access ad hoc networks. [Online]. Available: <http://arxiv.org/abs/0910.4704>
- [17] M. Wellens, J. Riihijärvi, and P. Mähönen, "Empirical time and frequency domain models of spectrum use," *Elsevier Physical Communication Journal*, vol. 2, no. 1–2, pp. 10–32, Mar.–Jun. 2009.
- [18] E. C. Y. Peh, Y.-C. Liang, Y. L. Guan, and Y. Zeng, "Optimization of cooperative sensing in cognitive radio networks: A sensing-throughput tradeoff view," *IEEE Trans. Veh. Technol.*, vol. 58, no. 9, pp. 5294–5299, Nov. 2009.
- [19] S. H. Song, K. Hamdi, and K. B. Letaief, "Spectrum sensing with active cognitive systems," *IEEE Trans. Wireless Commun.*, vol. 9, no. 6, pp. 1849–1854, June 2010.
- [20] L. Luo, N. M. Neihart, S. Roy, and D. J. Allstot, "A two-stage sensing technique for dynamic spectrum access," *IEEE Trans. Wireless Commun.*, vol. 8, no. 6, pp. 3028–3037, June 2009.
- [21] W. S. Jeon, D. G. Jeong, J. A. Han, G. Ko, and M. S. Song, "An efficient quiet period management scheme for cognitive radio systems," *IEEE Trans. Wireless Commun.*, vol. 7, no. 2, pp. 505–509, Feb. 2008.
- [22] D. Qu, Z. Wang, and T. Jiang, "Extended active interference cancellation for sidelobe suppression in cognitive radio OFDM systems with cyclic prefix," *IEEE Trans. Veh. Technol.*, vol. 59, no. 4, pp. 1689–1695, May 2010.
- [23] Z. Yuan and A. M. Wyglinski, "On sidelobe suppression for multicarrier-based transmission in dynamic spectrum access networks," *IEEE Trans. Veh. Technol.*, vol. 59, no. 4, pp. 1998–2006, May 2010.
- [24] P. Sutton, B. Özgül, I. Macaluso, and L. Doyle, "OFDM pulse-shaped waveforms for dynamic spectrum access," in *Proc. IEEE DySPAN*, Singapore, Apr. 6–9, 2010.
- [25] E. Reihl, "Wireless microphone characteristics," IEEE, Tech. Rep. 802.22-06/0070r0, May 2006.
- [26] D. Lam, D. C. Cox, and J. Widom, "Teletraffic modeling for personal communication services," *IEEE Commun. Mag.*, vol. 35, no. 2, pp. 79–87, Feb. 1997.
- [27] *Electromagnetic Compatibility and Radio Spectrum Matters (ERM); Technical Characteristics for Professional Wireless Microphone Systems (PWMS); System Reference Model*, ETSI Std. TR 102 546 v1.1.1, Apr. 2007.